

29 **Table of abbreviations**

30

BM	Base material
ACW	Asbestos containing wastes
CAPEX	Capital investment costs
CED	Cumulative energy demand
CO₂-eq	Equivalent CO ₂ emissions
CSP	Concentrated solar power
DSC	Differential scanning calorimeter
ECES	Energy conservation through energy storage
FA	Fly ashes
FT-IR	Infrared spectroscopy
GHG	Greenhouse gases
GWP	Global warming potential
h	Heat storage capacity
HTF	Heat transfer fluid
IACW	Intertized asbestos containing wastes
IEA	International Energy Agency
IP	Impact points
LCA	Life cycle assessment
MDSC	Modulated differential scanning calorimeter
MWCNT	Multi-walled carbon nanotubes
NFPA	National fire protection association
OPEX	Operation and maintenance costs
PCM	Phase change material
PT	Parabolic trough
SM	Stirring method
ST	Solar tower
SWCNT	Single walled carbon nanotubes
TES	Thermal energy storage
T_m	Temperature of fusion
TSSM	Two-step solution method
XR	X-ray powder diffraction

31

32 **1. Introduction**

33

34 Current trends in energy supply and demand are economically, environmentally and socially
35 unsustainable since energy-related emissions of carbon dioxide are expected to be doubled by
36 2050 and fossil energy demand is expected to be increased over the security of supplies [1]. The
37 International Energy Agency (IEA) recognizes energy storage technologies as a tool to support
38 energy security and climate change goals by helping to integrate electricity and heat systems.

39

40 Among the different energy storage technologies, thermal energy storage (TES) is an effective
41 technique that has become a key factor on improving the efficiency of different energy systems
42 due to the versatility in correcting the mismatch between the energy demand and supply, and by
43 allowing the development and implementation of renewable energies. A clear example is TES in
44 solar power plants, where the excess of solar energy during the Sun-light period, is stored to be
45 further released during the periods when the solar energy is needed but not available, such as
46 cloudy or night-time periods.

47

48 There are basically three main techniques for TES: sensible, latent and thermochemical, being
49 the first two the most studied and developed by the researchers. In sensible heat storage, the
50 storing (or releasing) of thermal energy is linked to the temperature rising (or dropping) without
51 undergoing phase change, as a consequence of a change in the internal energy of the TES
52 material. In latent heat storage, the media stores (or releases) the thermal energy when it
53 undergoes phase change. Unlike sensible heat storage, latent heat storage has higher storage
54 density because the phase-transition enthalpy is much higher (usually more than 50-100 times)
55 [2]. Since the process is nearly isothermal, which means that the temperature barely increases
56 (or decreases), all the energy stored comes from the molecular restructuration that takes place
57 within the transition from one phase to the other. Finally, in thermochemical heat storage the
58 energy is stored (or released) after a reversible chemical reaction between two substances. It
59 means that once the heat is released due to a dissociation of a chemical product, it can be
60 recovered in almost its totality when the synthesis reaction takes place.

61

62 TES can be implemented in many different sectors and applications. Table 1 summarizes the
63 most known and studied TES storage applications for a range that comprises low and high
64 temperature (from -269 °C to around 1600 °C).

65

66
67

Table 1. Review of the potential TES storage applications and sectors, as well as their range of working temperatures.

Sector and application	Range of temperatures	Reference
1. Heating and cooling	From -40 °C to 350 °C	
<i>1.1. Cold production</i>	<i>From -40 °C to -10 °C</i>	[2,3]
<i>1.2. Space heating and cooling of buildings</i>	<i>From 18 °C to 28 °C</i>	[4,5]
<i>1.3. Heating and cooling of water</i>	<i>From 29 °C to 80 °C</i>	[4,6]
<i>1.4. Absorption refrigeration</i>	<i>From 80 °C to 230 °C</i>	[7]
<i>1.5. Adsorption refrigeration</i>	<i>From -60 °C to 350 °C</i>	[8]
2. Transportation	From -50 °C to 800 °C	
<i>2.1. Cabin heating and refrigeration</i>	<i>From -50 °C to 70 °C</i>	[9,10]
<i>2.2. Battery and electronic protection</i>	<i>From 30 °C to 80 °C</i>	[9,10]
<i>2.3. Exhaust heat recovery</i>	<i>From 55 °C to 800 °C</i>	[9,10]
3. Thermal protection	From -269 °C to 130 °C	
<i>3.1. Electronic devices thermal protection</i>	<i>From 25 °C to 45 °C</i>	[11]
<i>3.2. Chips thermal protection</i>	<i>From 85 °C to 120 °C</i>	[12]
<i>3.3. Data centers thermal protection</i>	<i>From 5 °C to 45 °C</i>	[13]
<i>3.4. Spacecraft electronics thermal protection</i>	<i>From -269 °C to 130 °C</i>	[14]
<i>3.5. Food thermal protection</i>	<i>From -30 °C to 121 °C</i>	[15]
<i>3.6. Biomedical applications</i>	<i>From -30 °C to 22 °C</i>	[16]
4. Industry	From 60 °C to 260 °C	[17,18]
5. Solar energy	From 20 °C to 565 °C	
<i>5.1. Solar cooling</i>	<i>From 60 °C to 250 °C</i>	[19,20]
<i>5.2. Solar energy storage</i>	<i>From 20 °C to 150 °C</i>	[20]
<i>5.3. Solar power plants</i>	<i>From 250 °C to 565 °C</i>	[21,22]
6. Desalination	From 40 °C to 120 °C	[23,24]
7. Industrial waste heat recovery	From 30 °C to 1600 °C	[25,26]

68

69 TES has been of high interest for the researchers in the last decade and therefore many papers
70 can be found in the literature dealing this topic, especially at mid-low temperatures (below 150
71 °C). For example, Zalba et al. [27] reviewed and classified phase change materials (PCM) from
72 -33 °C on and described some of their main applications. Pielichowska and Pielichowski [22]
73 updated this review including sensible materials. At higher temperatures the number of
74 publications is considerably fewer. Liu et al. [28] focused their review on PCM and possible
75 thermal performance enhancement techniques at temperatures higher than 300 °C. Over the
76 same temperature range worked Cárdenas and León [29] and Fernandes et al. [30], who defined

77 a suitable material selection and procedure, defined different applications for power generation,
 78 and reviewed some enhancement techniques focused on different thermophysical properties.
 79 Although most of these reviews mentioned some of the requirements presented in Table 2, none
 80 of them organized the information in a way that addresses each of the requirements in order to
 81 help the final user to identify the right TES material, technology, system and/or enhancement
 82 technique.

83

84 Table 2 classifies the different requirements that, according to the literature, TES materials and
 85 systems should accomplish for an optimum thermal, physical, kinetic, chemical, economical,
 86 technological, and environmental performance.

87

88 Table 2. Main requirements for selecting the suitable materials and systems focused on high temperature
 89 TES. The requirements which have an * correspond only to latent storage. Based on [27,31-33].

		Requirements	Reason
Material	Chemical	Long-term chemical stability	Keeping the initial thermochemical properties along the cycling periods
		No chemical decomposition	
		Compatibility with container materials and low reactivity to heat transfer fluids (HTFs)	Ensuring long lifetime of the container and the surrounding materials in case of leakage
		No fire and explosion hazard	Ensuring workplace safety
		No toxicity	Ensuring handling safety
		*No phase separation / Incongruent melting	Avoiding changes on the stoichiometric composition of melt
	Kinetic	*Small or no subcooling	Having the same melting/solidification temperature and avoiding heat release problems
		*Sufficient crystallization rate	Meeting the recovery system heat transfer demands
	Physical	High density	Minimizing the volume occupied by the TES material
		Low vapour pressure	Diminishing the mechanical and chemical stability requirements of the container or vessel
		*Small volume changes (low density variation)	
		*Favourable phase equilibrium	Possibility of using eutectic mixtures
	Thermal	High specific heat	Providing significant sensible heat storage
		High thermal conductivity in both solid and liquid states	Enhancing the heat transfer within the TES material by providing the minimum temperature gradients
		*Melting / solidification temperature in the desired operating temperature range	Ensuring the success of the charging and discharging processes within the operation conditions

Material/System		*High latent heat of transition per unit volume near temperature of use	Providing significant latent heat storage in small volumes
		*Congruent melting	Ensuring the complete melt of the TES material and their homogeneity
	Economic	Abundant and available	Being cheaper than other options
		Large lifetime	Avoiding replacements and maintenance during the lifetime of the TES system
		Cost effective	Being competitive in front other options
	Environmental	Low manufacturing energy	Reducing the environmental impact of the systems and accomplishing sustainable regulations and trends
		Easy recycling and treatment	
		Low CO ₂ footprint and use of by-products	
		Non-polluting	
	Technological	Operation strategy	Optimizing the processes by adapting them to limiting factors such as maximum loads, nominal temperatures and specific enthalpy drops in load
		Integration into the facility	
		Suitable heat transfer between the HTF and the storage medium (efficiency)	Enhancing the heat transfer from the TES material to the HTF and vice versa

90

91 The main objective of the present paper is to identify the main requirements that a TES system
 92 (sensible or latent) should accomplish at high temperature (> 150 °C) from the material and
 93 system point of view, and reviewing the literature available on this topic in order to find the
 94 research niches which can allow the researchers conducting their investigation.

95

96 This is the first review considering such a wide scope and therefore the authors have divided it
 97 into two parts. The first part consists of a revision of all the general requirements that a TES
 98 system should fulfil in order to be considered optimal (chemical, economic, environmental,
 99 kinetic, physical, technological, and thermal). The second part [34] is mainly focused on the
 100 study of the thermal conductivity enhancement techniques between the HTF and the TES
 101 material, by adding extended surfaces, and enhancing the thermal conductivity of the material
 102 itself, by combining it with highly conductive materials.

103

104 **2. Material requirements**

105

106 **2.1 Addressing chemical requirements**

107

108 Chemical requirements are very similar for sensible and latent heat storage materials (Table 2).
109 Candidate materials should have long-term chemical stability, no chemical decomposition,
110 should be compatible with the container materials and the HTF, non-toxic and non-flammable,
111 and they should present no phase segregation.

112

113 Any material is suitable for TES applications if it is chemically stable and does not degrade
114 after a number of repeated heating and cooling cycles, which means that it keeps almost the
115 same thermochemical properties than the beginning. Many authors reported the results from
116 their cycling tests in which the chemical stability was checked. Ferrer et al. [35] reviewed the
117 methodologies used to assess the cyclability of TES materials. They identified that the infrared
118 spectroscopy (FT-IR) analysis is the most widely technique used to study the chemical stability.
119 In addition, they also identified the parameters that need to be considered when performing
120 those tests: cycling equipment, characterization technique after the test, number of cycles, and
121 heating rate. Only four studies regarding high temperature TES materials have been found. Solé
122 et al. [36] studied the chemical stability of three high temperature sugar alcohols (d-mannitol
123 [$T_m = 166 - 176.9$ °C], myo-inositol [$T_m = 224 - 227$ °C] and galacticol [$T_m = 187 - 188.5$ °C])
124 using differential scanning calorimeter (DSC) and FT-IR analyses. Results showed a poor
125 stability of galacticol and d-mannitol and a good stability of myo-inositol. Moreover, it was
126 observed that the contact of the TES materials with oxygen was a variable that affected the
127 results of the study. Therefore, a TES system including these materials should be in an inert
128 atmosphere or in vacuum. Similarly, John et al. [37] studied the effect of the upper cycle
129 temperature on the thermal behaviour of galactitol in bulk thermal cycling for solar cookers.
130 They observed the same poor stability results than Solé et al. [36] and concluded that this TES
131 material is not suitable for the application proposed. Paul et al. [38] studied the chemical
132 stability of a eutectic mixture at a 30:70 molar ratio of galactitol and mannitol ($T_m = 153$ °C) via
133 DSC, X-ray powder diffraction (XR) and FT-IR spectroscopy analyses. Those techniques
134 confirmed that the combination of mannitol and galacticol showed good cyclic, thermal and
135 chemical stability compared to its individual components under nitrogen or air atmospheres.
136 Finally, Sun et al. [39] cycled 1000 times an aluminium-magnesium-zinc alloy ($T_m = 450$ °C).
137 Results showed a good stability of the alloy as it showed an 11% of loss on the heat storage
138 capacity and a variation of 0.7 % on the melting temperature.

139

140 The compatibility of the TES material and the container material is crucial in order to ensure a
141 long lifetime as a result of a minimum variation of its mechanical and structural properties. This
142 property is often assessed by measuring the corrosion between the TES and the container
143 materials. Corrosion is normally measured by immersing a sample made of the container

144 material in the liquid TES material. Temperature, length and repeatability of the analysis depend
145 on the specific requirements of the applications.

146

147 Table 3 shows a review of the corrosion studies performed at high temperature and defines the
148 TES and containers materials, working temperatures, results and year in which they were
149 performed. Eutectic mixtures containing sodium nitrate and potassium nitrate are the most
150 studied high temperature TES material because of their potential use in solar power plants. The
151 combination of molten salts and the metallic parts of the solar power plants constitutes a
152 corrosion system, where the salts act as an electrolyte, comparable to an aqueous electrolyte.
153 However, whereas the corrosion mechanisms of metals in numerous aqueous electrolytes are
154 well established and understood, it still exists a lack in knowledge concerning the corrosion
155 mechanisms of metals in molten salts [40]. The corrosion of different commercial steels and
156 other alloys are evaluated when in contact with nine different high temperature eutectic
157 mixtures used for TES. The corrosion tests have been performed at different working
158 temperature, ranging from 250 to 800 °C. However, different procedures (metal weight/gain
159 losses, corrosion rates, etc.) were used by those authors to evaluate the corrosion and, therefore,
160 it is not possible to perform an accurate comparison of the results reviewed. Moreover, the
161 compatibility between a TES material and its container cannot be transferred from the literature
162 straightforward. At the working conditions (temperature, length, intermittence, etc.) of the real
163 application in which those materials are expected to be used should be assessed. Guillot et al.
164 [41] assessed the suitability of combining intertised asbestos containing wastes (IACW), which
165 are industrial wastes based on calcium magnesium iron alumino-silicate with different
166 impurities, with molten salts to be combined and used as TES material in concentrated solar
167 power (CSP) plants. Sulphates, phosphates, carbonates and nitrates salts have been mixed with
168 IACW and the corrosion indicated that only the nitrates have shown good compatibility with
169 IACW materials.

Table 3. Review of the studies concerning the chemical requirements at high temperature in terms of compatibility between the container and the TES material.

Study case	TES material (wt %)	Container material	Working temperature	Results	Year	Reference	
1	(HITEC) NaNO ₂ + NaNO ₃ + KNO ₃ (40 % + 7 % + 53 %)	Steel	A516	390 °C	Mass gain = 0.35 mg/cm ²	2015	Fernandez et al. [42]
			T11	390 °C	Mass gain = 0.35 mg/cm ²		
			T22	390 °C	Mass gain = 0.35 mg/cm ²		
			321	530 °C	≈ 0.02 mm/a	2015	Federsel et al. [43]
		Other alloys	Inconel 600	530 °C	≈ 0.02 mm/a	2015	Federsel et al. [43]
			AISI 430	390 °C	< 0.1 mg/cm ²	2015	Fernandez et al. [44]
			T22	390 °C	0.00044 μm/h		
			A1	390 °C	0.00075 μm/h		
			SS316	550 °C	> 1 mg/cm ²	2004	Goods and Bradshaw [45]
				A36	550 °C		
SS304	390 °C		<0.1 mg/cm ²	2015	Fernandez et al. [44]		
	550 °C		< 3 mg/cm ²	2004	Goods and Bradshaw [45]		
3	KNO ₃ + NaNO ₃ (50 % + 50 %)	Other alloys	Inconel	677 °C	3.05-4.83 mm/a	1985	Slusser et al. [46]
			Hastelloy		3.30-10.41 mm/a		
			Alloy		4.32 mm/a		
			RA		6.86 mm/a		
			Incoloy		10.67 mm/a		
			Haynes		17.53-21.08 mm/a		
			Nitronic		21.33-29.72 mm/a		
			Nicofer		43.18 mm/a		
			Ni		81.79 mm/a		
4	(Molten salts) NaNO ₃ + KNO ₃ (60 % + 40 %)	Steel	SS304	390 °C	< 0.05 mg/cm ²	2014	Fernandez et al. [47,48]
				550 °C	0.0062 μm/h		
				570 °C	4-10 mg/cm ²	2004	Goods and Bradshaw [45]
		T11	390 °C	2.75 mg/cm ²	2014	Fernandez et al. [49]	
		T22	390 °C	0.0081 μm/h	2014	Fernandez et al. [48]	
			550 °C	2.25 mg/cm ²		Fernandez et al. [50]	
		OC-4	390 °C	Excellent behaviour	2014	Fernandez et al. [47]	
A1	390 °C	0.1108 μm/h	2014	Fernandez et al. [48]			

			A36	316 °C	1-2.5 mg/cm ²	2004	Goods and Bradshaw [45]
			AISI SS430	390 °C	0 mg/cm ²	2014	Fernandez et al. [50]
				550 °C	0.1321 μm/h		Fernandez et al. [48]
			P91	600 °C	Scale thickness = 1330 μm	2016	Dorcheh et al. [51]
			X20	600 °C	Scale thickness = 450 μm	2016	Dorcheh et al. [51]
			SS316	570 °C	5-8 mg/cm ²	2004	Goods and Bradshaw [45]
				600 °C	Scale thickness = 18 μm	2016	Dorcheh et al. [51]
			316Ti	565 °C	≈ 0.5 % weight loss	2015	Federsel et al. [43]
			SS347H	600 °C	Scale thickness = 18 μm	2016	Dorcheh et al. [51]
			SS321	400 °C	Descaled loss = 0.27 mg/cm ²	2014	Kruizenga and Gill [52]
				500 °C	Descaled loss = 1.98 mg/cm ²	2014	Kruizenga and Gill [52]
				565 °C	≈ 0.2 % weight loss	2015	Federsel et al. [43]
				680 °C	Descaled loss = 42.77 mg/cm ²	2014	Kruizenga and Gill [52]
			SS347	400 °C	Descaled loss = 0.2 mg/cm ²	2014	Kruizenga and Gill [52]
		500 °C		Descaled loss = 1.28 mg/cm ²	2014	Kruizenga and Gill [52]	
		680 °C		Descaled loss = 42.05 mg/cm ²	2014	Kruizenga and Gill [52]	
		Other alloys	HA230	600 °C	Metal losses of 23.6 μm/a	2014	McConohy and Kruizenga [53]
				680 °C	Metal losses of 688 μm/a	2014	McConohy and Kruizenga [53]
			In625	600 °C	Scale thickness = 9 μm	2016	Dorcheh et al. [51]
				600 °C	Metal losses of 16.8 μm/a	2014	McConohy and Kruizenga [53]
				680 °C	Metal losses of 594 μm/a.	2014	McConohy and Kruizenga [53]
Incoloy Alloy 800	550-670 °C		Oxide scales higher than 15 μm	1981	Goods [54]		
5	LiNO ₃ + NaNO ₃ + KNO ₃ (30 % + 18 % + 52 %)	Steel	SB450	550 °C	n.a.	2015	Cheng et al. [55]
			T22	550 °C	n.a.		
			T5	550 °C			
			T9	550 °C			
			X20	550 °C			

6	Molten salts with NaCl additives	Stainless steel	304	570 °C	7-10 mg/cm ²	2004	Goods and Bradshaw [45]
			316	570 °C	5-6 mg/cm ²		
		Carbon steel	A36	316 °C	2-3 mg/cm ²		
7	(FLiNaK) LiF + NaF + KF (46.5 % + 11.5 % + 42 %)	Steel	SS316L	650 °C	19.65 mm/a	2014	Sona et al. [56]
			SS317L		17.82 mm/a		
			Inconel-625		23.70 mm/a		
			Incoloy-800H		39.30 mm/a		
			Hasteloy-B		3.02 mm/a		
			Ni-201		0.94 mm/a		
8	NaCl + KCl (50 % + 50 %)	Fe-Cr alloy	n.a.	670 °C	n.a.	2005	Li et al. [57]
		Fe-Al alloy					
		Ni-Al alloy					
		Steel	316L	670 °C	n.a.	2010	Abramov et al. [58]
			316Ti				
			321				
9	NaCl + KCl + ZnCl ₂ (13.4 % + 33.7 + 52.9 %)	Hastelloy	C-276	500 °C	Corrosion rate < 20 μm/a	2015	Vignarooban et al. [59]
				800 °C	Corrosion rate 40 μm/a		
			C-22	250 °C	Corrosion rate < 20 μm/a		
				500 °C	Corrosion rate 40 μm/a		
		Stainless steel	304	250 °C	Corrosion rate 20 μm/a		
				500 °C	Corrosion rate 380 μm/a		

n.a: not available

In order to facilitate the handling and the safe use of the TES material, no hazardous materials are preferable. Therefore toxic or flammable TES materials should be avoided. However, most of the authors have focused only on the thermal behaviour properties when selecting TES materials without taking into account those parameters. Miró et al. [60] proposed health hazard as a part of a new methodology to select the suitable TES materials. Moreover, a case study considering five high temperature PCMs (salicylic acid, benzanilide, d-mannitol, hydroquinone, and potassium thiocyanate) was presented. The degree of health hazard of a material is based on the form or condition of the material and on its inherent properties. It is provided by the manufacturer in the material safety data sheets or by different standard associations which have developed tools to indicate the health, flammability, reactivity and special hazards for many common chemicals [60]. Results showed that potassium thiocyanate was the most dangerous TES materials within the selected ones and its short exposure could cause serious temporary or moderate residual injuries. TES material with health hazard values above 3 (according to the National fire protection association (NFPA) 704 standard in a scale from 0 to 4) should be discarded. However, if a specific application requires it, its use must be always under the established safety measures. In Table 4, the health hazard rating of the different materials studied are presented. Regarding to the flammability, Gallegos and Yu [61] proposed TES as and insulation medium in high temperatures systems when the heat flux presented values up to 80-84 kW·m⁻² from flashover conditions in a firefighting environment. Among the proposed candidates, they analysed dulcitol and d-mannitol. Results showed that the molecular structure of sugar alcohols has tremendous impacts in terms of melting and boiling point and therefore in flammability.

Table 4. Health hazard rating of some TES materials based on the NFPA 704 standard [60].

	Health hazard rating
Salicylic acid	½
Benzanilide	1
d-mannitol	1
Hydroquinone	2
Potassium thiocyanate	3

Phase segregation (or phase separation) is the macroscopic separation of the phases in a PCM. When that occurs, PCM shows a significantly lower capacity to store heat [33]. According to Zhao [62], encapsulation can help to mitigate not only phase segregation during thermal cycling but also problems like low thermal conductivity and subcooling. Moreover, it protects the TES material from exposure and potential corrosion with HTF. Therefore, the encapsulation material should also be compatible with the TES material. Metals are the best candidates for

39 encapsulation at high temperature due to their properties such as strength, thermal conductivity,
40 wear resistance, excellent workability and ductility [62,63]. However, the use of shells and their
41 characteristics are strongly determined by the volumetric expansion of the material and the
42 pressure increase during the melting process [64]. In order to avoid problems such as chemical
43 corrosion and thermal stress, the use of ceramic shells is starting to gain relevance [65]. A more
44 detailed review on shell materials used in the encapsulation of TES materials for high
45 temperature is presented in Jacob and Bruno [66].

40

41 2.2 Addressing kinetic requirements

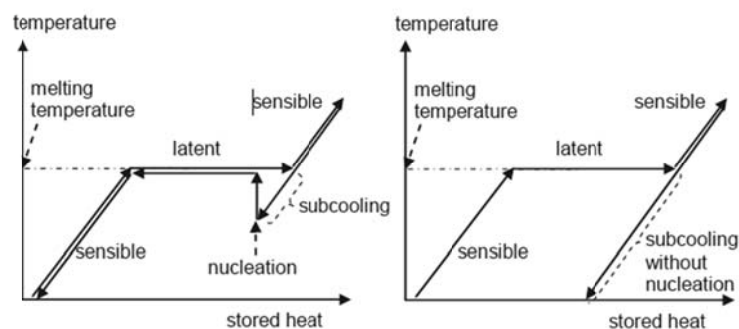
42

47 The kinetic requirements identified in this review include small or no subcooling during the
48 solidification in order to have the similar temperatures in both the melting and the solidification
49 processes and therefore avoiding heat release problems, and sufficient crystallization rate in
50 order to meet the recovery system heat transfer demands. These two requirements are referred
51 only to latent heat storage systems [67].

48

53 In the literature, only research work discussing the subcooling effect is found. This effect, also
54 known as supercooling or undercooling [33], refers to a solidification process which does not
55 start immediately upon cooling below the melting temperature, but starts the crystallization only
56 after a temperature well below the melting temperature (Fig. 1). It appears mostly in inorganic
57 PCM.

54



55

56 Fig. 1. Effect of subcooling on heat storage. Left: little subcooling and nucleation, right:

57

severe subcooling without nucleation [33].

58

62 The most common approach to eliminate the subcooling effect is the addition of additives, also
63 known as nucleating agents, into the TES material in order to cause heterogeneous nucleation.
64 Most of the nucleating agents are materials with a similar crystal structure than the solid TES
65 material, which allows the solid phase of the TES material to grow on their surface but with

62 higher melting temperature to avoid deactivation when the TES material is melted. The main
63 problem of this solution is that similar crystal structures usually means similar melting
64 temperatures.

65

66 Very little research has been carried out regarding kinetics at high temperature. For example,
67 Sari et al. [68] reduced the subcooling of galacticol ($T_m = 187.4\text{ }^\circ\text{C}$) by preparing galactitol
68 hexastearate and galactitol hexapalmitate as a novel solid–liquid TES material by means of
69 esterification reaction of the TES material with palmitic acid and stearic acid. However, this
70 mixture led to a TES material with a melting temperature of around $40\text{ }^\circ\text{C}$. Paul et al. [38]
71 studied the effect of adding up to 0.5 wt.% of different nucleating agents (graphite and silver
72 iodide) into an eutectic mixture at a 30:70 molar ratio of galactitol and mannitol ($T_m = 153\text{ }^\circ\text{C}$).
73 They observed that the nucleation agents reduced subcooling around $10\text{ }^\circ\text{C}$. Other studies
74 observed that the size of the sample is an important parameter when determining the subcooling
75 effect [69-71]. Rathgeber et al. [69] selected nine TES materials for combined DSC and T-
76 history measurements. From these materials, hydroquinone was the only one at high
77 temperature. Using both DSC and T-history for the determination of enthalpy curves, the
78 dependence of this curve on the sample size and on the temperature profile applied could be
79 analysed and a reduction of around $13\text{ }^\circ\text{C}$ in the subcooling effect was observed. Gil et al. [70]
80 tested at both laboratory and pilot plant scales two TES materials candidates for solar
81 refrigeration applications (hydroquinone and d-mannitol). They realized that d-mannitol showed
82 subcooling in both scales while hydroquinone showed subcooling only at laboratory scale. Later
83 on, both materials were also analysed with the T-History method [71], verifying that the effect
84 of subcooling was volume-dependent.

85

86 **2.3 Addressing physical requirements**

87

88 Regarding the physical requirements, TES materials should have high density in order to
89 decrease the space needed to store the same amount of heat. In addition, low vapour pressure
90 and low density variation between phases are needed to diminish the mechanical and chemical
91 stability requirements of the container. Finally, and specifically for TES materials working in
92 their latent phase, favourable phase equilibrium is required.

93

94 Despite the fact that these parameters are very important when designing the TES container or
95 the encapsulation for the TES material, there is a paucity of literature on this requirement at
96 high temperature. Regarding the low density variation, Archiblod et al. [71] and Solomon et al.
97 [73] considered the thermal expansion coefficient of sodium nitrate ($T_m = 306.8\text{ }^\circ\text{C}$) and the
98 effect of an internal air void when evaluating its thermal performance within a metallic spherical

99 shell. They highlighted that the salt quantity inside the sell should be carefully calculated to
100 guarantee the internal pressure. Moreover, they found that the shape of the melting front and the
101 rate at which it moves is affected by the location of the internal air void. Hennemann et al. [74]
102 studied the physical laws limiting the heat of fusion and the usability of TES material in
103 applications, and an exhaustive study of entropy was done regarding expansional, positional,
104 orientational, conformational and electronic contribution of entropy. They concluded that
105 disregarding molecules with molecular weights less than 70 g/mol, the limiting theoretical
106 entropy value set by physical and chemical constrains was 1.0 J/(g·K).

107

108 **2.4 Addressing thermal requirements**

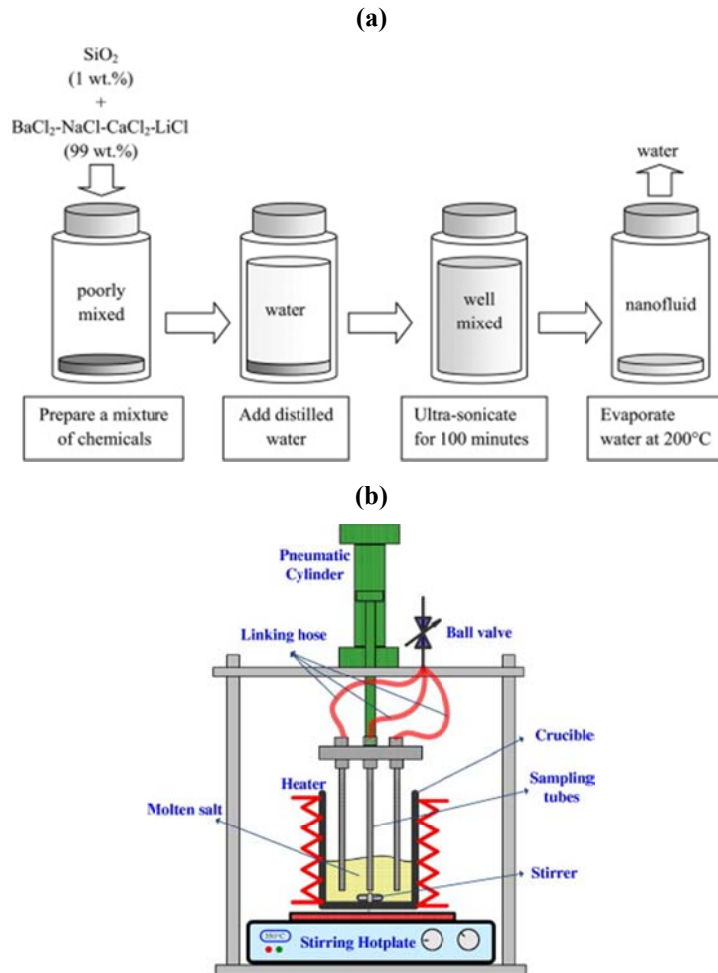
109

110 It is a fact that most of the materials used for TES purposes have poor thermal characteristics
111 and therefore enhancement techniques addressing these requirements need to be performed. As
112 Table 2 shows, there are five main thermal requirements that TES materials should meet in
113 order to optimize the processes in which they are planned to be implemented. If the thermal
114 storage is requested to occur in the latent phase, TES materials must have their phase change
115 temperature in the desired operating temperature range in order to increase the potential of the
116 system. Moreover, high latent heat of transition per unit volume near the temperature of use is
117 also desired in order to provide significant latent heat storage with small volumes and therefore,
118 obtaining lower operation costs due to the optimization of the storage container. The last
119 thermal requirement regarding the use of the latent phase is the utilization of a TES material
120 with congruent melting in order to ensure that it completely changes of phase and therefore,
121 both solid and liquid phases remain homogeneous. These three parameters can be evaluated
122 with commercial devices.

123

124 On the contrary, most of TES materials employed for high temperature purposes are used in
125 their sensible phases. Hence, laboratory analyses should be performed in order to determine the
126 proper thermal properties and optimize them within the desired operation temperature range.
127 The first requirement is that the TES material should have high thermal conductivity at both
128 solid and liquid states. This requirement, which has received a high interest from the
129 researchers, is fully reviewed and developed in the second part of this review [34]. The second
130 requirement is that the TES material should have high specific heat to provide significant
131 sensible heat storage. Normally, TES materials used for high temperature purposes have low
132 specific heat. The most widely used technique to enhance this property is the dispersion of
133 nanoparticles within the TES material. As mentioned in the second part of this review [34], the
134 material composed by nanoparticles dispersed within a base material (BM) is usually presented
135 as nanofluid, when the BM is in the liquid state, or nanocomposite, when the BM is in the solid

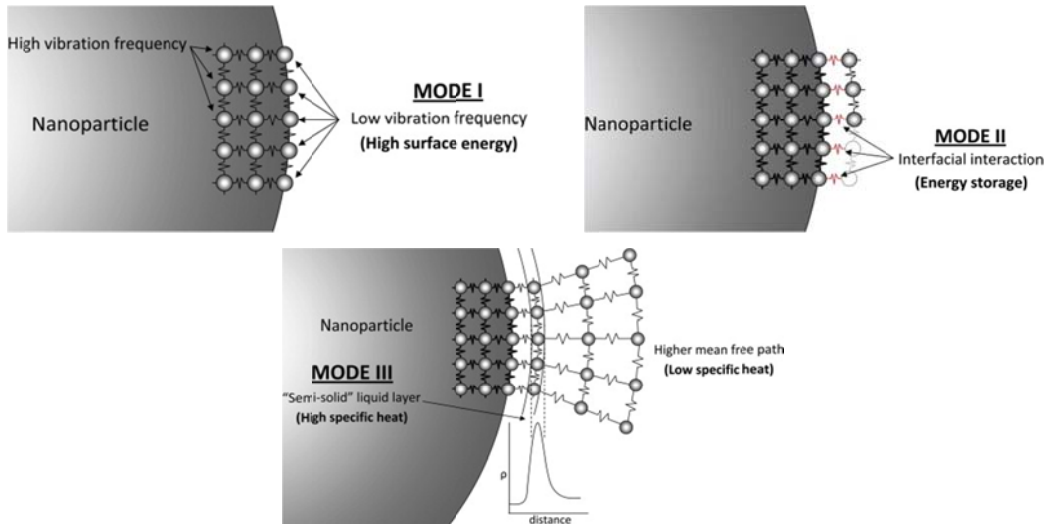
139 state. Both nanofluids and nanocomposites can be obtained from two different synthesis
 140 methods [75] (Fig. 2): the two-step solution method (TSSM) or liquid solution method [76] and
 141 the stirring method (SM) [77].
 140



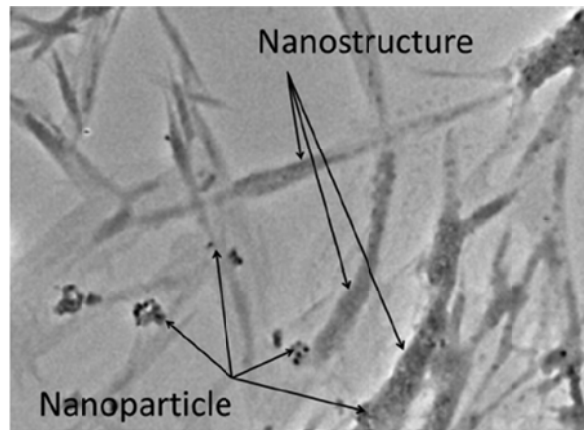
142 Fig. 2. Obtainment of nanomaterials at high temperature: (a) Schematic diagram of preparation of the two
 143 step solution method [76]. (b) Schematic diagram of preparation of the stirring dispersion method [77].
 143

153 Despite the fact that this enhancement technique for high temperature purposes is still in the
 154 early stages of research, several studies have been carried out since 2011. Controversial results
 155 were found on these studies. It has been observed that while in the water-based and organic-
 156 based nanomaterials an increase on the specific heat was not achieved if compared to the pure
 157 material (following the traditional thermal equilibrium model) [78], in the molten salt-based
 158 nanomaterials an increase of the specific heat was observed. Shin and Banerjee [76] proposed
 159 three mechanisms to help to understand these anomalous enhancements: low vibration
 160 frequency, interfacial interaction and higher mean free path (Fig. 3). Shin and Banerjee [79]
 161 went a step further and detailed why the molten salts nanofluids do not follow the conventional
 162 effective specific heat model based on thermal equilibrium, but followed a more complex one.

158 The reason lied on the fact that the molten salts mixtures are formed by different ionic
 159 compounds, which have different electrostatic interaction with the nanoparticles. Therefore,
 160 when the nanoparticles are dispersed into the molten salts mixture, the different compounds are
 161 separated near nanoparticles, due to the above-mentioned difference in the electrostatic
 162 interaction and crystallize forming a fractal-like nanostructure (Fig. 4).
 159



161 Fig. 3. Three transport mechanisms proposed to understand the anomalous enhancement with
 162 nanomaterials [76].
 162



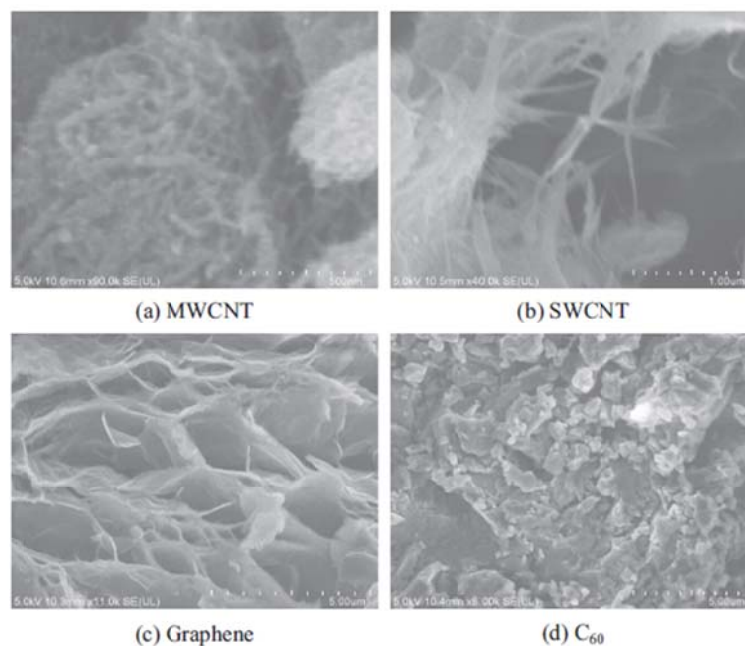
163 Fig. 4. Microscope view of nanoparticles and fractal-like nanostructures [79].
 164
 165

172 Practically all the different studies carried out DSC analysis to evaluate the specific heat of the
 173 nanomaterial and it is being proved that the results obtained from such analysis need to be
 174 carefully treated [80]. Table 5 reviews, in a chronological order, the different studies carried out
 175 concerning the specific heat enhancement technique of dispersing nanoparticles with TES
 176 materials at high temperature, by showing the TES material acting as BM, the nanoparticles
 177 materials, the dimension and concentration of nanoparticles, the method of synthesis, the
 178 improvement obtained and the measurement instrument.

173

192 Regarding these experimental studies, the two TES material which have been selected the most
193 as base materials to test the specific heat enhancement because of the dispersion of
194 nanoparticles heat have been the eutectic mixtures of sodium nitrates and potassium nitrates,
195 and the eutectic mixtures of lithium carbonates and potassium carbonates. The different authors
196 have studied the influence of the concentration of nanoparticles (from 0.5 to 4.6 wt %) [75,77,81,82,84-87,89],
197 of the influence of the nanoparticles material (mica, SiO₂, Al₂O₃, TiO₂,
198 SiO₂-Al₂O, carbon nanotubes, graphene and fullerene C₆₀ (Fig. 5)) [82,86,87], and of the
199 influence of the particle size (5, 10, 30 and 60 nm) [83,84,88]. The lack of standards for the
200 preparation, the measurement and the evaluation of the results, as well as the lack of knowledge
201 of the behaviour of the composite at nano-scale, generates an elevated uncertainty which
202 currently makes very difficult the exercise of obtaining proper conclusions. However, Table 5
203 shows that the highest specific heat enhancement was achieved with a nanoparticle
204 concentration of 1 wt.%. Regarding the particle size, there is no significant variation in the
205 specific heat enhancement. Therefore, the fact of having the nanoparticles well-dispersed within
206 the BM rather than agglomerated might be one of the parameters responsible of such
207 enhancement. Ho and Pan [77] obtained the minimum concentration value at which
208 nanoparticles starts to aggregate and it turned to be 0.016 wt.%. Therefore, a standardization of
209 the preparation and evaluation of both the nanomaterial and the results, as well as, studies with
210 samples containing masses higher than the studied at laboratory scale, should be considered.

193



194

195

Fig. 5. Carbon nanostructures obtained by SEM analysis [87].

Table 5. Review of the studies concerning the combination of nanoparticles with TES material at high temperature in terms of specific heat enhancement.

Study case		Nanoparticle (nominal size)	Nanoparticles concentration (wt. %)	TES material (wt %)	Synthesis method	Comparison	Improvement and measurement instrument	Year	Reference
1	Experimental	Al ₂ O ₃ (50 nm)	0.5/1.0/2.5	[C ₄ mmim][NTf ₂]	n.a.	Concentration of nanoparticles	Up to 30.4 % (2.5 wt. %)	2011	Bridges et al. [90]
2	Experimental	Mica (45 μm)	0.5/1.0/2.0	KNO ₃ + NaNO ₃ (60 + 40 %)	TSSM	Concentration of nanoparticles	Up to 15 % (1.0 wt. %, solid state). Up to 19 % (1.0 wt. %, liquid state)	2011	Jung and Banerjee [81]
							By: MDSC (Q20, TA Instruments)		
3	Experimental	SiO ₂ (20-30 nm)	1.0	BaCl ₂ + CaCl ₂ + LiCl + NaCl (15.9 + 34.5 + 29.1 + 20.5 %)	TSSM	Nanomaterial vs pure material	Up to 14.5 %	2011	Shin and Banerjee [76]
							By: MDSC (Q20, TA Instruments)		
4	Experimental	TiO ₂ (20-30 nm)	1.0	Li ₂ CO ₃ + K ₂ CO ₃ (62 + 38 %)	TSSM	Nanomaterial vs pure material	Up to 23 %	2011	Shin and Banerjee [91]
							By: MDSC (Q20, TA Instruments)		
5	Experimental	SiO ₂ (7 nm) Al ₂ O ₃ (13 nm) TiO ₂ (20 nm) SiO ₂ -Al ₂ O ₃ (2-	0.5/1.0/1.5	NaNO ₃ + KNO ₃ (60 + 40 %)	TSSM	Nanoparticle and concentration of nanoparticles	SiO ₂ : Up to 14.9 % (1.0 wt. %, solid state). Up to 0.8 % (1.0 wt. %, liquid state)	2013	Chieruzzi et al. [82]

		200 nm)					<p>Al_2O_3: Up to 19.9 % (1.0 wt %, solid state). Up to 5.9 % (1.0 wt. %, liquid state)</p> <p>TiO_2: No enhancement observed</p> <p>$SiO_2-Al_2O_3$: Up to 57.7 % (1.0 wt. %, solid state). Up to 22.5 % (1.0 wt. %, liquid state)</p> <p>By: Mettler-Toledo DSC 822E/400</p>		
6	Experimental	SiO_2 (5/10/30/60 nm)	1.0	$NaNO_3 + KNO_3$ (60 + 40 %)	TSSM	Size of nanoparticles	<p>Up to 10 % (1.0 wt. %, 60nm, solid state). Up to 28 % (1.0 wt. %, 60nm, liquid state)</p> <p>By: MDSC (Q20, TA Instruments)</p>	2013	Dudda and Shin [83]
7	Experimental	Al_2O_3 (13/90 nm)	0.9/2.7/4.6	$NaNO_3 + KNO_3$ (60 + 40 %)	TSSM	Concentration of nanoparticles and particle size	<p>No enhancement observed</p> <p>By: MDSC (Q20, TA Instruments)</p>	2013	Lu and Huang [84]
8	Experimental	SiO_2 (2-20 nm)	1.5	$Li_2CO_3 + K_2CO_3$ (62 + 38 %)	TSSM	Nanomaterial vs pure material	Up to 54 % (solid state). Up to 124 % (liquid state)	2013	Shin and Banerjee

							By: MDSC (Q20, TA Instruments)		[92]
9	Experimental	SiO ₂ (5/10/30/60 nm)	1.0	Li ₂ CO ₃ + K ₂ CO ₃ (62 + 38 %)	TSSM	Size of nanoparticles	Up to 28 % (60 nm, solid state). Up to 26 % (60nm, liquid state)	2013	Tiznobaik and Shin [93]
							By: MDSC (Q20, TA Instruments)		
10	Experimental	SiO ₂ (12 nm)	0.5/1.0/1.5/2.0	NaNO ₃ + KNO ₃ (60 + 40 %)	TSSM	Concentration of nanoparticles	Up to 25 % (1.0 wt. %).	2014	Andreu-Cabedo [75]
							By: Mettler-Toledo DSC 822E/400		
11	Experimental	Al ₂ O ₃ (<50 nm)	0.016/0.063/0.125/0.25/0.5/1.0/2.0	KNO ₃ + NaNO ₂ + NaNO ₃ (53+ 40 + 7 %)	SM	Concentration of nanoparticles	Up to 19.9 % (0.063 wt. %)	2014	Ho and Pan [77]
							By: Perkin Elmer/DSC 7		
12	Experimental	Sn/SiO ₂ (100 nm)	1.0/3.0/5.0	KNO ₃ + NaNO ₃ (40 + 60 %) KNO ₃ + NaNO ₂ + NaNO ₃ (53 + 40 + 7 %)	n.a.	Concentration of nanoparticles	<i>KNO₃+NaNO₃</i> : Up to 36.3 % (5.0 wt. %).	2014	Lai et al. [89]
							<i>KNO₃+NaNO₂+NaNO₃</i> : Up to 30.1 % (5.0 wt. %).		
							By: Mettler-Toledo DSC 822E/400		
13	Experimental	SiO ₂ (60 nm)	1.0	LiNO ₃ + NaNO ₃ + KNO ₃ (38 + 15 + 47 %)	TSSM	Nanomaterial vs pure material	Up to 33 %	2014	Seo and Shin [94]
							By: MDSC (Q20, TA Instruments)		
14	Experimental	Al ₂ O ₃	1.0	Li ₂ CO ₃ + K ₂ CO ₃	TSSM	Nanomaterial vs	Up to 33 %	2014	Shin and

		(60 nm)		(62 + 38 %)		pure material	By: MDSC (Q20, TA Instruments)		Banerjee [95]
15	Experimental	MWCNT (10-30 nm x 1.5µm)	1.0	Li ₂ CO ₃ + K ₂ CO ₃ (62 + 38 %)	TSSM	Nanomaterial vs pure material	Up to 16 % (solid state). Up to 21 % (liquid state) By: MDSC (Q20, TA Instruments)	2014	Jo and Banerjee [96]
16	Experimental	SiO ₂	1.0	Li ₂ CO ₃ + K ₂ CO ₃ (62 + 38 %)	TSSM	Nanomaterial vs pure material	Up to 15 % (solid state) By: MDSC (Q20, TA Instruments)	2015	Shin and Banerjee [97]
17	Experimental	Al ₂ O ₃ (40 nm)	0.125/0.25/0.5/0.75/1.0/1.5/2.0	NaNO ₃ + KNO ₃ (60 + 40 %)	TSSM	Concentration of nanoparticles	Up to 30.6 % (0.78 wt. %) By: MDSC (Q20, TA Instruments)	2015	Schuller et al. [85]
18	Experimental	SWCNT (5-20 nm x 1-5 µm) MWCNT (10-50 nm x 0.5-1 µm) Graphene (10-20 nm x 1-5 µm) Fullerene C ₆₀ (0.5-2 µm)	0.1/0.5/1.0/1.5/2.0 .5	Li ₂ CO ₃ + K ₂ CO ₃ (62 + 38 mol %)	TSSM	Nanoparticle and concentration of nanoparticles	SWCNT: Up to 18.7 % (1.5 wt. %, solid state). Up to 14.4 % (1.5 wt%, liquid state) MWCNT: Up to 12.4 % (1.5 wt. %, solid state). Up to 14.52 % (1.5 wt. %, liquid state) Graphene: Up to 16.8 % (1.5 wt. %, solid state). Up to 18.57 % (1.5 wt. %, liquid state)	2015	Tao et al. [87]

							C_{60} : Up to 13.47 % (2.5 wt. %, solid state). Up to 12.05 % (2.5 wt. %, liquid state)		
							By: n.a.		
19	Experimental	SiO ₂ (7 nm) Al ₂ O ₃ (13 nm) SiO ₂ -Al ₂ O ₃ (2-200 nm)	1.0	KNO ₃	TSSM	Nanoparticle	SiO ₂ : Up to 9.5 % (solid state). Up to 6.1 % (liquid state) Al ₂ O ₃ : No enhancement observed SiO ₂ -Al ₂ O ₃ : Up to 4.7 % (solid state). No enhancement observed in the liquid state By: Mettler-Toledo DSC 822E/400	2015	Chieruzzi et al. [86]
20	Experimental	SiO ₂ (5/10/30/60 nm)	1.0	LiNO ₃ + NaNO ₃ + KNO ₃ (38 + 15 + 47 %)	TSSM	Size of nanoparticles	Up to 16 % (10 and 30 nm) By: MDSC (Q20, TA Instruments)	2016	Seo and Shin [88]
21	Experimental	SiO ₂ (30 nm)	1.0	NaNO ₃ + KNO ₃ + Ca(NO ₃) ₂ (49 + 30 + 21 %)	TSSM	Nanomaterial vs pure material	Up to 19 % By: MDSC (Q20, TA Instruments)	2016	Devaradjan e and Shin [98]

MDSC: Modulated differential scanning calorimeter / *SWCNT*: Single walled carbon nanotubes / *MWCNT*: Multi-walled carbon nanotubes / *TSSM*: Two-step solution method / *SM*: Stirring method

3. System requirements

3.1 Addressing economic requirements

A common problem in the current research field is that TES is mainly focused on the analysis of the intrinsic properties of the materials and its enhancement techniques and the system requirements (Economy, technology and environment) are sometimes ignored. The economic feasibility of a TES system is assessed taking into account parameters like abundance and availability of the TES material, large lifetime of the components and cost effectiveness.

Most of the economic analyses are focused on CSP facilities as they are one of the most developed technologies at the high temperature range. More than 80% of CSP plants which are already built or under construction are based on the parabolic trough technology [106]. Hence, practically all the information regarding economic aspects refers to this technology. CSP facilities costs are mainly divided in three categories: capital investment costs (CAPEX), operation and maintenance costs (OPEX) and financing costs [107]. It is very difficult to obtain feasible and real values, since very few information is currently available because of confidentiality. Table 6 shows the breakdown of the CAPEX costs of two proposed 100 MW CSP plants in South Africa. The first one corresponds to a parabolic through CSP plant with 13.4 h of storage and estimated total CAPEX costs of 914 million USD, while the second one corresponds to a solar tower CSP plant with 15 h of TES and estimated total CAPEX costs of 978 million USD. In both cases the most economic-intensive part is the solar and heliostat field, representing one third of the total investment. From this cost, the elements made of steel and the mirrors are the largest contributors. On the other hand, the TES system represents 10-15 % of the total cost, being the TES material and the storage tanks the largest contributors. OPEX costs include the replacement costs of the damaged and broken elements of the plant, the water costs for mirror washing, and insurance among others, and have values between 0.020 and 0.036 USD/kWh for parabolic trough CSP plants, and around 65 USD/kW/year for solar tower CSP plants [106]. Finally, the authors of the study reviewed potential CSP cost reduction potentials and identified the following potential innovations: new HTFs, new storage materials, new mirror material and new collector concepts.

Table 6. Breakdown of the CAPEX of two proposed 100 MW CSP plants in South Africa [107].

Section	CAPEX breakdown	
	Parabolic trough CSP	Solar tower CSP
Solar field / Heliostat field	35 %	33 %

Site preparation	n.a.	4 %
Tower	n.a.	2 %
Receiver system	n.a.	15 %
Owner's costs	5 %	5 %
Contingencies	8 %	8 %
Engineering	7 %	6 %
Balance of plant	6 %	6 %
Power block	17 %	11 %
TES system	15 %	10 %
HTF system	7 %	-

Wagner and Rubin [109] combined the cost with the performance and the profit of a 110-MW parabolic trough CSP plant operating with a TES system, with and without natural gas-fired backup system. The use of TES was found to increase the annual capacity factor and the total plant capital costs but decreased the annual operation and maintenance costs. Nithyanandam and Pitchumani [110] studied, in terms of cost and performance, two different TES systems types (encapsulated PCM and embedded heat pipes) integrated in tower CSP plants, and compared them with the results of a two-tank molten salt storage system. Results showed that the costs of integrating the two-tank molten salt storage system is at least 1.12 €/kWh and 0.71 €/kWh higher compared to encapsulated PCM and embedded heat pipes systems, respectively.

Regarding to other types of TES systems, Rathgeber et al. [111] evaluated the storage capacity costs ($\text{€}\cdot\text{kWh}^{-1}$) of different TES systems from the participants institutions at Energy conservation through energy storage (ECES) Annex 29 via top-down and bottom-up approaches. Some of the systems presented work at high temperature. Results showed that the annual number of storage cycles has the largest influence on the cost effectiveness.

3.2 Addressing environmental requirements

As environmental awareness increases, industries and businesses are assessing how their activities affect to the environment. Table 2 lists the environmental requirements for a whole TES system (TES material, container, piping system, insulation, etc.). These requirements aim to reduce the environmental impact of the TES systems and to accomplish sustainable regulations and trends. Therefore it is desirable to have a low manufacturing energy demand, to demand an easy recycling and treatment, and to use non-polluting and low CO₂ footprint materials. These requirements can be assessed by performing environmental analyses and/or using by-products or industrial wastes as alternative TES materials.

Regarding the environmental analysis, three main tools have been found focused on identifying the environmental affection of those systems: the carbon or CO₂ footprint, the life cycle assessment (LCA), and the cumulative energy demand (CED). The CO₂ footprint measures the greenhouse gases (GHG) emissions over the whole life of a product from the extraction of raw materials and manufacturing right through to its use and final re-use, recycling or disposal [112]. It considers direct emissions, which are emissions from sources that are owned or controlled by the reporting entity, and indirect emissions, which are emissions that are a consequence of the activities of the reporting entity, but occur at sources owned or controlled by another entity. In fact, the CO₂ footprint is a simplification of the LCA analysis, and instead of considering all the impact categories a LCA (Table 7), it only considers the global warming impact category. LCA analyses the impact of a product from the extraction, through manufacturing, transportation and use, to its disposal. LCA divides the environmental burdens analysis into three different damage categories: human health, ecosystem quality and resources. Finally, the CED considers direct and indirect energy use throughout the life cycle, including the energy consumed during the extraction, manufacturing and disposal of the raw and auxiliary materials [113].

Table 7. Main impact categories of LCA classified by scale impact and their quantification, based on [114].

	Impact category	Quantification
Global impact	Global warming	CO ₂ -Eq
	Resource depletion	$\frac{\text{Quantity resource used}}{\text{Quantity left in reserve}}$
	Ozone depletion	CFC-11 equivalents
Regional impact	Smog	Ethane equivalents
	Acidification	Hydrogen ion equivalents
Local impact	Eutrophication	PO ₄ equivalents
	Human toxicity	LC50 equivalents
	Ecotoxicity	LC50 equivalents
	Land use	Mass of solid waste
	Water use	$\frac{\text{Quantity water used}}{\text{Quantity left in reserve}}$

The environmental analyses found in the literature are classified in this review depending on the boundaries of the study. First, only the TES material. Afterwards, the TES system (it includes

the HTF, the container material and the insulation). Finally, the whole facility (it includes the TES system and the heating and cooling systems).

Considering only the TES material, Khare et al. [115] identified some sensible heat storage materials to work from 500 °C on and calculated their environmental affection during the different life cycle stages. Among all the materials studied, they observed that high alumina concrete was the less energy requiring material and with the lower values of CO₂ production as a consequence of little material processing and local transport. López-Sabirón et al. [116] performed an LCA to determine whether the energy savings of conventional fuels during the operation stage were large enough to balance the environmental impact of four different latent TES system (used to recover thermal energy in a temperature range from 300 °C to 400 °C) from its manufacture to its disposal. Results showed a reduction in the overall impacts by the use of TES. Besides, they also calculated the carbon footprint of the main integrating components of these TES system. They observed that the HTF is the lowest contributor while the steel and the PCM are the highest contributors. In another study, López-Sabirón et al. [117] evaluated a TES system with PCM including the manufacture, use and end-of-life stages. They observed that changing the materials in the manufacture of the TES, raising the material recovery ratios, and selecting the proper HTF, can increase the positive impact of the end-of-life stage.

Regarding both the material and system, Oró et al. [118] compared the LCA of three different TES systems for solar power plants: sensible heat storage (concrete and molten salts) both in solid and liquid thermal storage media and latent heat storage (molten salts). They concluded that the system containing sensible liquid thermal storage media was the one with higher environmental impact. The same systems were analysed by Miró et al. [119], who besides accounted their CED. In this case, results showed that the latent system was the one accounting for more embodied energy. Recently, Lalau et al. [120] compared the environmental impacts of a thermocline TES system using Cofalit as the filler material to a conventional two-tank molten salt TES system. The authors used the global warming potential (GWP), CED and water indicators to calculate the Cofalit manufacturing impact. They identified a reduction in comparison with the two-tank molten salt storage of 40 % for the GWP, 30 % for the CED and 60 % for water. Moreover, the advantages of using Cofalit are its availability and its high working temperature (up to 1000 °C).

Finally, from the point of view of the whole facility, Klein [121] analysed the water consumption, land use, and life cycle GHG emissions of different backup cooling options (wet and dry cooling combined with fossil fuels or molten salts TES) by applying a multi-criteria

decision analysis to a 1 MWh parabolic trough CSP plant. In this study, the authors suggested a preference for the TES backup. In another study, Klein and Rubin [122], applied an LCA analysis to the same CSP plant than Klein [121] and considered also different backup systems. They concluded that facilities with TES have less GHG emissions than plants using natural gas as backup system but higher land use. Lechón et al. [123] performed an LCA analysis of two solar thermal plants located in Spain using molten salts as TES material: one with the solar tower technology (17 MW) and the other with the parabolic trough technology (50 MW). They accounted for 634 kt of CO₂ savings if thermal power objectives for Spain were accomplished. Giuliano et al. [124] accounted and compared the CO₂ emissions of five 30 MW solar-hybrid plants (with and without molten salts as storage system) to a conventional fossil-fired driven plant. Results showed that larger solar fields and the integration of TES reduced the CO₂ emissions up to 68% if compared to the fossil-fired combined cycle. Whitaker et al. [125] analysed the GHG emissions, water consumption and CED of a 106 MW solar tower CSP plant. They compared the origin of the TES material (mined or synthetic) and the configuration of the storage system (two-tank or thermocline). They concluded that the use of synthetic salts increased the cumulative energy demand and the switching from two-tank to thermocline configuration was insignificant regarding all the environmental parameters. The same environmental analysis was used by Burkhardt et al. [126] in a parabolic trough CSP plant (103 MW). In this case, the same conclusion than Burkhardt et al. [126] was achieved regarding the origin of the TES material. In addition, the authors found a 7 % of GHG emissions reduction when using thermocline instead of two-tank configuration.

Table 8 shows the different studies found in the literature concerning the environmental analysis at high temperature. It is classified according to the TES material and ordered chronologically. Besides, the type of environmental analysis performed and the software and database used are also listed. It can be seen that there is a lack of environmental analysis in systems containing TES materials, since only twelve cases have been found in the literature. Among them, molten salts are the most studied TES material in the high temperature range considered in this article (> 150 °C). Other materials studied are sodium nitrate, high temperature concrete, ferrous metals, alumina, high alumina concrete, graphite, magnesia and silicon carbide. In order to perform the different environmental analyses, EcoInvent and SimaPro are the most used software. Regarding to the parameters analysed, LCA and CO₂ footprint are the ones which have been calculated more often. Generally, when TES is evaluated and compared to conventional systems from a material point of view, its benefits are not significant. However, when the comparison is done at system level and at higher scale, the benefits of introducing TES, such as a reduction of CO₂ emissions, and energy and water consumption, are more noticeable. On the contrary, the main disadvantage is the land use.

Table 8. Review of the studies concerning the environmental analysis at high temperature.

Study case	Boundary	TES material	Parameter analysed	Software / Database used	Results	Year	Reference
1	Facility	Molten salts	LCA	SIMAPRO	ST: 9.49 g CO ₂ -eq/kWh PT: 14.60 g CO ₂ -eq/kWh	2008	Lechón et al. [123]
2	Facility	Molten salts	CO ₂ emissions reduction	n.a.	ST: 0.062-0.414 kg CO ₂ -eq/kWh PT: 0.098-0.482 kg CO ₂ -eq/kWh	2011	Giuliano et al. [124]
3	Facility	Molten salts	CO ₂ footprint	SIMAPRO	5.01-5.21 g CO ₂ eq/kWh	2011	Burkhardt et al. [126]
			Water consumption	EcoInvent database	0.19 L/kWh		
			CED		0.07 MJ/kWh		
4	Material and system	Molten salts (sensible)	LCA	Eco-Indicator 99	3376 IP	2012	Oró et al. [118]
		Molten salts (latent)			1270 IP		
		High temperature concrete			279 IP		
5	Material	Magnesium Aluminium Zinc Al+Si (88+12 wt %) Al+Mg+Zn (60+34+6 wt %)	Energy consumption CO ₂ footprint	CES EcoAudit™	Energy and CO ₂ production for the alloy 88Al–12Si being the lowest, followed by aluminium	2013	Khare et al. [115]
6	Facility	Molten salts	Water consumption	SIMAPRO	0.73-5 L/kWh	2013	Klein [121]
			Land use		240-286 m ² /GWh		
			CO ₂ footprint		49-73 g CO ₂ -eq/kWh		

7	Facility	Molten salts	Water consumption	n.a.	2.3-2.4 L/kWh	2013	Klein and Rubin [122]
			Land use		n.a.		
			CO ₂ footprint		0.33-0.34 kg CO ₂ -eq/kWh		
8	Facility	Mined and synthetically derived molten salts	CO ₂ footprint	SIMAPRO EcoInvent database	The use of synthetic salts increase CO ₂ footprint 12%, CED by 7%, and water consumption by 4% compared to mined salts	2013	Whitaker et al. [125]
			Water consumption				
			CED				
9	Material	KNO ₃ NaOH K ₂ CO ₃ +Na ₂ CO ₃ +Li ₂ CO ₃ (35+33+32 wt %) LiOH+KOH (40+60 wt %)	CO ₂ footprint	EcoInvent database Simapro	LiOH/KOH benefits -8 to -18 ton CO ₂ eq in comparison with other cases	2014	López-Sabirón et al. [116]
10	Material	Sodium nitrate	LCA	SIMAPRO CML 2001 Eco-Indicator 99	n.a.	2014	López-Sabirón et al. [117]
11	Material and system	Molten salts (sensible)	CED	EcoInvent database	125 TJ	2015	Miró et al. [119]
		Molten salts (latent)			257 TJ		
		High temperature concrete			17 TJ		
12	Material and system	Cofalit	GWP	CML 2001	2.4 kg CO ₂ -eq/kWh	2016	Lalau et al. [120]
			CED		0.046 MJ/kWh		
			Water consumption		0.058 L/kWh		

LCA: Life cycle assessment / *CED*: Cumulative energy demand / *GWP*: Global warming potential / *ST*: Solar tower / *PT*: Parabolic trough / *CO₂-eq*: Equivalent CO₂ emissions / *IP*: Impact points

1 Regarding the use of by-products and industrial wastes to reduce environmental impact of TES
2 systems, researchers have proposed the use of waste materials and by-products from different
3 industries as TES materials in order to reduce the environmental impact of the facilities which
4 contains a TES system [127]. The use of these materials reduces significantly the environmental
5 impact if compared to other manufactured products as they avoid both extraction of raw
6 materials and manufacturing life cycle stages. Moreover, if these materials do not need any
7 further treatment, they are considerably cheaper. Some examples of by-products and waste
8 materials candidates for high temperature TES purposes are: Intertized asbestos containing
9 wastes (ACW), fly ashes (FA), by-products from the salt and metal industry and municipal
10 wastes.

11
12 Several authors [128-131] studied the recycled industrial ceramics made of ACW. Results
13 showed that this material presented no hazard, no environmental impact, good thermophysical
14 properties and very low investment cost. Meffre et al. [132] studied and characterized FA as
15 TES material. FA are micron-size particles present in gaseous effluents produced by industrial
16 combustions in facilities such as coal fired power plants or municipal solid wastes incinerators.
17 They are mainly composed of SiO_2 , Al_2O_3 and CaO and its waste treatment is also generally
18 performed by plasma torch processing [133]. Results from the characterization showed good
19 thermophysical properties for sensible TES storage and an energy payback of the plasma torch
20 waste treatment of 7.4 months for CSP applications. By-products from the salt industry were
21 studied by Miró et al. [134] and Ushak et al. [135]. The authors performed thermophysical and
22 morphological characterisation at laboratory scale, and evaluated their performance at pilot
23 plant scale. It was found that this by-product had high potential for commercial TES up to a
24 temperature of 200 °C but corrosion should be previously solved. The steel industry produces
25 different types of by-products (referred as slags) depending on the furnace technology used.
26 Thermo-physical properties of ferrous slag [139-142] indicate very appropriate values for the
27 use of this material in sensible thermal energy storage up to temperatures of 1200 °C. Finally,
28 some authors proposed mixtures of wastes and TES materials. For example, Ozger et al. [137]
29 proposed nylon fibres from post-consumer textile carpet waste for fibre-reinforced concrete as
30 candidate for high temperature sensible heat storage up to 450 °C, and Navarro et al. [138]
31 proposed by-products from the copper industry to be mixed with cement.

32
33 Table 9 lists the by-products which have been currently studied by different researchers and the
34 temperature at which they have been tested. However, researchers do not only focus on by-
35 products because of their environmental advantages but also focus on these products from the
36 economical point of view, since they are usually cheaper than current TES materials.

38 Table 9. Summary of the studies concerning the environmental requirements at high temperature in terms
 39 of potential by-products and waste materials candidates for TES purposes.

Study Case	By-product	Temperature range analysed	Year	Reference
1	Asbestos containing wastes (ACW)	Up to 1000 °C	2000-2014	Py et al. [128] Kere et al. [129] Gualtieri and Tartaglia [130] Calvet et al. [131]
2	Fly ashes (FA)	Up to 1100 °C	2011-2012	Meffre et al. [132]
3	NaCl from salt industry	100-200 °C	2014	Miró et al. [134]
4	Astrakanite from salt industry	570-680 °C	2014	Ushak et al. [135]
5	Ferrous slag from metal industry	Up to 1200 °C	2011-2014	Gil et al. [139] Ortega et al. [140,141] Mills [142]

40

41 3.3 Addressing technological requirements

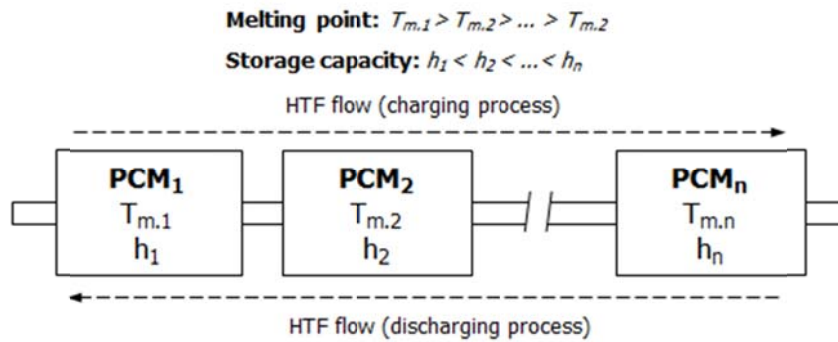
42

43 Technological requirements, which include the integration of the TES material into the facility,
 44 the operation strategy of the facilities, and the good transfer between the HTF and the TES
 45 material, are not usually considered in the literature, even though these requirements are known
 46 to have an incidence in the design and the economics of the system. The integration of the TES
 47 material into the facility can help TES systems to be considered as substitutes of conventional
 48 fossil-fuel technologies. A good operation strategy can considerably enhance the overall TES
 49 system heat transfer efficiency, which is closely linked to the requirement of good heat transfer
 50 between the HTF and the TES material. Finally, the most important operation strategies
 51 containing TES at high temperature are the multiple PCMs configuration and the forced
 52 movement of the TES material while undergoing phase change.

53

54 Multiple PCMs configuration, also referred as cascaded or multistage configuration, is a TES
 55 system configuration where different PCMs (with different melting temperatures and
 56 enthalpies) are arranged in series. This configuration aims to increase low storage capacities in
 57 the single PCM due to the poor PCM thermal conductivities. As it can be observed in Fig. 6, the
 58 optimum arrangement for a multiple PCM system is obtained by placing the PCMs in a
 59 decreasing order of their melting temperatures (T_m) and in an increasing order of their heat
 60 storage capacities (h) in the HTF flow direction during the charging process, and the other way
 61 around during the discharging process [143]. The advantages of this arrangement are the

66 increase of the heat transfer rate during charging and discharging, especially in the latent part,
 67 the uniform and higher outlet HTF temperature for a longer period during charging and
 68 discharging process, the faster charging and discharging process, the increase of exergy
 69 efficiency and the increase of average effectiveness.



68
 69 Fig. 6. Optimum arrangement of a multiple PCM system [143].

70
 76 Hence, in order to achieve the greatest performance improvement, researchers need to study the
 77 thermophysical properties of the candidate PCMs with the aim of not selecting them arbitrarily
 78 but select the suitable combination and with the proper dimensions for the desired application.
 79 Tao et al. [144] performed an optimization of the PCM temperatures for a two-stage PCM
 80 storage unit using the entransy theory and Li et al. [145] optimized the geometrical parameters
 81 of their proposed storage unit.

77
 86 In the literature, few multiple PCMs configuration within the high temperature range are found.
 87 Gong and Mujumdar [146] used five PCM in the range 667 – 867 °C, Cui et al. [147] three
 88 PCM in the range 717 – 779 °C, Michels and Pitz-Paal [148] used three PCM in the range 306 –
 89 335 °C, Seeniraj and Lakshmi Narasimhan [149] used five PCM in the range 873 – 767 °C,
 90 Shagbard et al. [150] used three PCM in the range 318 – 370 °C, Li et al. [145] used three PCM
 91 in the range 397 – 710 °C, Tao et al. [144] used two PCM in the range 746 – 767 °C, Wang et al.
 92 [151] used three PCM in the range 390 – 485 °C and finally Peiró et al. [143] used two PCM in
 93 the range 158.5 – 168.5 °C. Most of them are numerical studies [144-147,149-151] and only two
 94 experimental cases have been found [143,148].

87
 89 Table 10 summarizes the characteristics of the multiple PCM configuration analysis found in
 90 the literature and their improvement versus single PCM configuration.

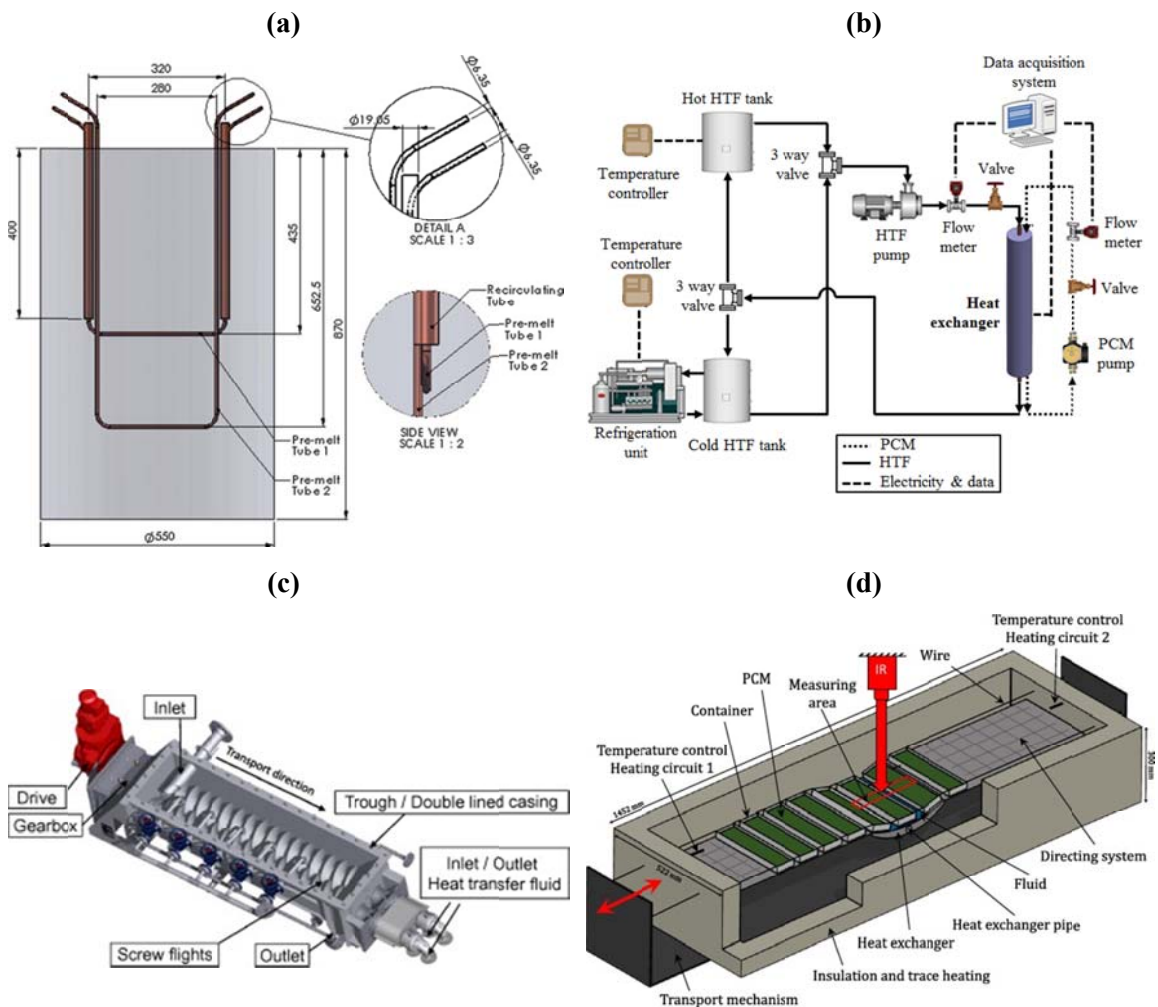
90

Table 10. Review of the studies concerning the technological requirements at high temperature in terms of numerical and experimental analysis of cascaded PCM configurations.

Study case		Heat exchanger design	Number of PCM	TES materials (mol%) and order in which they are placed	Melting temperature	Improvement vs single configuration	Year	Reference
1	Numerical	Single pass shell and tube	5	1. n.a.	1. 867 °C	More uniform HTF outlet temperature	1995	Gong and Mujumdar [146]
				2. n.a.	2. 817 °C			
				3. LiF + CaF ₂ (80.5 + 19.5 %)	3. 767 °C			
				4. n.a.	4. 717 °C			
				5. n.a.	5. 667 °C			
2	Numerical	Single pass shell and tube	3	1. n.a.	1. 779 °C	Reduction of the HTF outlet temperature variations Energy rate enhancement	2003	Cui et al. [147]
				2. LiF + CaF ₂ (80.5 + 19.5 %)	2. 767 °C			
				3. n.a.	3. 717 °C			
3	Experimental	Single pass shell and tube	3	1. KNO ₃	1. 335 °C	Reduction of the HTF outlet temperature variations Energy rate enhancement	2007	Michels and Pitz-Paal [148]
				2. KNO ₃ + KCl (95.5 + 4.5 %)	2. 320 °C			
				3. NaNO ₃	3. 306 °C			
4	Numerical	Single pass shell and tube	5	1. LiF + CaF ₂ (80.5 + 19.5 %)	1. 767 °C	Reduction of the HTF outlet temperature variations Energy rate enhancement	2008	Seeniraj et al. [149]
				2. Eutectic mixture LiF-MgF ₂	2. 736 °C			
				3. n.a.	3. 700 °C			
				4. n.a.	4. 650 °C			
				5. n.a.	5. 600 °C			
5	Numerical	Rectangular container with HTF flow channels	3	1. NaOH + NaCl (73.3 + 26.7 %)	1. 370 °C	Increase 10 % exergy recovery	2012	Shagbard et al. [150]
				2. KCl + MnCl ₂ + NaCl (22.9 + 60.6 + 16.5 %)	2. 350 °C			

		located at the top and bottom		3. NaOH + NaCl + Na ₂ CO ₃ (65.2 + 20 + 14.8 %)	3. 318 °C			
6	Numerical	Single pass shell and tube	3	1. K ₂ CO ₃ + Na ₂ CO ₃ (51 + 49 %)	1. 710 °C	No comparison with single configuration has been done in this study	2013	Li et al. [145]
				2. Li ₂ CO ₃ + NaCO ₃ + K ₂ CO ₃ (20 + 60 + 20 %)	2. 550 °C			
				3. Li ₂ CO ₃ + NaCO ₃ + K ₂ CO ₃ (32 + 33 + 35 %)	3. 397 °C			
7	Numerical	Single pass shell and tube	2	1. LiF + CaF ₂ (80.5 + 19.5 %)	1. 767 °C	Energy rate enhancement Reduction of the entransy dissipation rate	2014	Tao et al. [144]
				2. LiF + MgF ₂ (67 + 33 %)	2. 746 °C			
8	Experimental	Multiple pass shell and tube	2	1. Hydroquinone	1. 168.5 °C	Higher uniformity on the outlet HTF temperature Effectiveness enhancement of 19.36 %	2015	Peiró et al. [143]
				2. D-mannitol	2. 158.5 °C			
9	Numerical	Zig zag configuration	3	1. n.a.	1. 450, 460, 470, 480, 485 °C	Intensification of the charging process	2015	Wang et al. [151]
				2. n.a.	2. 440 °C			
				3. n.a.	3. 395, 400, 410, 420, 430 °C			

16 Despite the fact that very little investigation has been carried out at high temperature, a novel
 17 heat transfer enhancement technique between the TES material and the HTF is included in this
 18 review, which is known as forced movement of the TES material while undergoing phase
 19 change. Three different concepts are currently dealing with this technique: dynamic melting
 20 [152,153], screw heat exchanger [154] and PCM flux [155] (Fig. 7). They mainly consist of
 21 moving the TES material during the phase change processes with an external force (transport
 22 mechanism or pump). As a consequence, there is a dominance of the forced convection heat
 23 transfer mechanism during the melting process, which increases the overall heat transfer
 24 coefficient and therefore, the heat transfer between the HTF and the TES material. During the
 25 solidification process, this technique continuously avoids the presence of a solid layer around
 26 the heat transfer surface by removing it, which decreases the thermal resistance of the material.
 27 Three main advantages can be identified in this enhancement technique: first, the heat transfer
 28 can be controlled by adjusting the HTF and PCM velocities; second, the phase segregation can
 29 be prevented because of the forced movement; third, the packing factor, which is the ratio
 30 between the volume of PCM and the volume of the TES container, is maintained constant.
 17



17 Fig. 7. Prototypes of the concepts dealing with the forced movement of the TES material while
 18 undergoing phase change: (a) and (b) Dynamic melting [152,153]; (c) screw heat exchanger [154]; (d)
 19 PCM flux [155]

20
 21 Finally, a good heat transfer between the HTF and the TES material is desired in order to
 22 enhance both the charging and discharging processes. The most common and widely used HTF
 23 for high temperature purposes are listed with their maximum operation temperature and, when
 24 possible, with their reported price in Table 11.

25
 26 Table 11. Cost and maximum operation temperature of the most commonly used HTFs.

Heat transfer fluid	Max. operation temperature	Cost*	Reference
1. Liquids			
1.1. Molten salts			
Hitec XL	500 °C	1.19-1.66 USD·kg ⁻¹	[99]
Hitec	535-538 °C	0.93-1.93 USD·kg ⁻¹	[100,101]
Solar salt	585-593 °C	0.49-1.30 USD·kg ⁻¹	[100,101]
Other nitrate mixtures	565 °C	≈ 1.1 USD·kg ⁻¹	[99]
Other carbonate mixtures	850 °C	≈ 1.3 USD·kg ⁻¹	[99]
Other chloride mixtures	850 °C	0.35-1.13 USD·kg ⁻¹	[99]
Other fluoride mixtures	900 °C	7-14 USD·kg ⁻¹	[99]
Other oxide mixtures	1200 °C	n.a	[100]
1.2. Thermal oils			
Commercial brands	280-400 °C	2.83-105.4 USD·L ⁻¹	
1.3. Liquid glasses			
Liquid glasses	450 °C	n.a.	[101]
1.4. Liquid metals			
1.4.1. Alkali metals			

NaK (22.2 wt. % Na + 77.8 wt. % K)	785 °C	2 USD·kg ⁻¹	[102]
K	766 °C	2 USD·kg ⁻¹	[102]
Na	873-883 °C	2 USD·kg ⁻¹	[99-101]
Li	1342 °C	60 USD·kg ⁻¹	[102]
1.4.2. Heavy metals			
Lead-bismuth eutectic allow (LBE) (44.5 wt. % Pb + 55.5 wt. % Bi)	1533-1670 °C	13 USD·kg ⁻¹	[99,101,102]
Pb	1743 °C	2 USD·kg ⁻¹	[102]
Bi	1670 °C	22 USD·kg ⁻¹	[102]
1.4.3. Fusible metals			
Ga	2237 °C	600 USD·kg ⁻¹	[102]
In	2072 °C	500 USD·kg ⁻¹	[102]
Sn	2687 °C	25 USD·kg ⁻¹	[102]
2. Supercritical fluids			
Supercritical H ₂ O	620 °C	n.a.	[101]
Supercritical C ₂ O	850 °C	n.a.	[101]
3. Gases			
Superheated steam	600 °C	0	[101]
Compressed air	800 °C	0	[100]

*Commercial cost at May 2015 without shipping fees

27

28

29 Two research groups studied how to improve the thermal conductivity of commercial HTF in
30 order to increase the heat transfer rates between HTFs and TES materials. Cingarapu et al. [103]
31 dispersed 5 vol.% of core/shell silica encapsulated tin (Sn/SiO₂) nanoparticles in Therminol66,
32 obtaining an enhancement of 11 %. Torres-Mendieta et al. [104] dispersed spherical gold
33 nanoparticles in Therminol VP-1 and obtained an enhancement of 4 %. Other authors have also
34 proposed the lead-bismuth eutectic alloy PbBi and molten tin [102], and dense particle
35 suspension (DPS) fluidized with air [105] for candidates as HTF.

36

37 4. Conclusions

38

39 In the part 1 of this article, the requirements that TES materials and TES system should
40 accomplish for an optimal performance and a widespread deployment are reviewed. High
41 temperature is considered above 150 °C and only latent and sensible TES are studied. These

42 requirements are divided depending if they are focused on the TES material or on both the TES
43 material and system. Requirements focused on the TES material are grouped into chemical,
44 physical and thermal while the requirements focused on the TES material and systems are
45 grouped into environmental, economic and technologic. Part 2 of this article presents a review
46 of the numerical and experimental studies focused on the different thermal conductivity
47 enhancement techniques in the high temperature range.

48

49 The most studied topics regarding the different requirements reviewed are:

50 ▪ **Materials requirements**

51 The full characterization of the TES material is very important to assess its suitability
52 for a TES application.

53 ○ *Chemical*

54 This is the most studied requirement regarding the TES material. Long-term
55 stability, compatibility between TES materials and their surrounding
56 components (especially for solar salts and metals used in solar power plants),
57 phase segregation and handling and safe use of the materials are assessed in the
58 literature.

59 ○ *Kinetic*

60 Few studies have been found regarding the identification of the subcooling
61 effect dealing with galacticol, hydroquinone and d-mannitol.

62 ○ *Physical*

63 Thermal expansion coefficient is found to be basic for design purposes.
64 Therefore, the TES material quantity inside the TES container and/or shell
65 capsule should be carefully calculated to guarantee the internal pressure and
66 avoid leakages.

67 ○ *Thermal*

68 The main thermal requirement is the enhancement of the thermal conductivity,
69 which is widely reviewed in Part 2 of this review. Regarding the rest of
70 requirements, increasing the specific heat by including nanoparticles is the most
71 attractive research topic.

72 ▪ **Material and system requirements**

73 These requirements are not directly related to the TES material but are basic for the
74 design of the facility.

75 ○ *Economic*

76 Most of economic analyses are focused on CSP facilities and the capital
77 investment costs (CAPEX), operation and maintenance costs (OPEX) and

78 financing costs are studied. Moreover, the annual number of storage cycles has
79 the largest influence on the cost effectiveness.

80 ○ *Environmental*

81 Carbon footprint, Life Cycle Assessment and Cumulative Energy Demand
82 analyses have been developed at three different scales (TES material, TES
83 system and the whole facility). Most of them consider solar power plants.
84 Moreover, the use of by-products or industrial wastes has been assessed.

85 ○ *Technological*

86 Multiple PCMs configuration and the forced movement of the TES material
87 while undergoing phase change ~~dynamic melting systems~~ have been proposed
88 by the researchers as important strategies for maximizing the heat transfer
89 between the HTF and the TES material.

90

91 **Acknowledgments**

92

93 The work is partially funded by the Spanish government (ENE2015-64117-C5-1-R, ENE2011-
94 22722 and ULLE10-4E-1305). The authors would like to thank the Catalan Government for the
95 quality accreditation given to their research group GREA (2014 SGR 123). This project has
96 received funding from the European Commission Seventh Framework Programme (FP/2007-
97 2013) under Grant agreement N°PIRSES-GA-2013-610692 (INNOSTORAGE) and from the
98 European Union's Horizon 2020 research and innovation programme under grant agreement No
99 657466 (INPATH-TES). Laia Miró would like to thank the Spanish Government for her
100 research fellowship (BES-2012-051861). Jaume Gasia would like to thank the Departament
101 d'Universitats, Recerca i Societat de la Informació de la Generalitat de Catalunya for his
102 research fellowship (2016FI_B 00047).

103

104 **References**

- 105 1. International Energy Agency. Technology Roadmap: Energy storage 2014.
106 2. Wongsuwan W, Kumar S, Neveu P, Meunier F. A review of chemical heat pump
107 technology and applications. *Appl Therm Eng* 2001;21:1489–519. doi:10.1016/S1359-
108 4311(01)00022-9.
109 3. Meunier F. Solid sorption: An alternative to CFCs. *Heat Recovery Syst CHP*
110 1993;13:289–95. doi:10.1016/0890-4332(93)90051-V.
111 4. Cabeza LF, Castell A, Barreneche C, de Gracia A, Fernández AI. Materials used as
112 PCM in thermal energy storage in buildings: A review. *Renew Sustain Energy Rev*
113 2011;15:1675–95. doi:10.1016/j.rser.2010.11.018.
114 5. Zhang Y, Zhou G, Lin K, Zhang Q, Di H. Application of latent heat thermal energy
115 storage in buildings: State-of-the-art and outlook. *Build Environ* 2007;42:2197–209.
116 doi:10.1016/j.buildenv.2006.07.023.

- 117 6. Mazman M, Cabeza LF, Mehling H, Nogues M, Evliya H, Paksoy HÖ. Utilization of
 118 phase change materials in solar domestic hot water systems. *Renew Energy*
 119 2009;34:1639–43. doi:10.1016/j.renene.2008.10.016.
- 120 7. Srihirin P, Aphornratana S, Chungpaibulpatana S. A review of absorption refrigeration
 121 technologies. *Renew Sustain Energy Rev* 2001;5:343–72. doi:10.1016/S1364-
 122 0321(01)00003-X.
- 123 8. Demir H, Mobedi M, Ülkü S. A review on adsorption heat pump: Problems and
 124 solutions. *Renew Sustain Energy Rev* 2008;12:2381–403.
 125 doi:10.1016/j.rser.2007.06.005.
- 126 9. Johnson RW, Evans JL, Jacobsen P, Thompson JR, Christopher M. The changing
 127 automotive environment: high-temperature electronics. *IEEE Trans Electron Packag*
 128 *Manuf* 2004;27:164–76. doi:10.1109/TEPM.2004.843109.
- 129 10. Jankowski NR, McCluskey FP. A review of phase change materials for vehicle
 130 component thermal buffering. *Appl Energy* 2014;113:1525–61.
 131 doi:10.1016/j.apenergy.2013.08.026.
- 132 11. Patapoutian A, Peier AM, Story GM, Viswanath V. ThermoTRP channels and beyond:
 133 mechanisms of temperature sensation. *Nat Rev Neurosci* 2003;4:529–39.
 134 doi:10.1038/nrn1141.
- 135 12. Kandasamy R, Wang X-Q, Mujumdar AS. Application of phase change materials in
 136 thermal management of electronics. *Appl Therm Eng* 2007;27:2822–32.
 137 doi:10.1016/j.applthermaleng.2006.12.013.
- 138 13. ASHRAE Technical Committee (TC) 9.9. 2011 Thermal Guidelines for Data
 139 Processing Environments – Expanded Data Center Classes and Usage Guidance 2011.
- 140 14. Larson WJ, Wertz JR, editors. *Space Mission Analysis and Design*. 3rd edition. El
 141 Segundo, Calif. : Dordrecht ; Boston: Microcosm; 1999.
- 142 15. Dincer I. *Heat Transfer In Food Cooling Applications*. CRC Press; 1997.
- 143 16. Mondieig D, Rajabalee F, Laprie A, Oonk HAJ, Calvet T, Angel Cuevas-Diarte M.
 144 Protection of temperature sensitive biomedical products using molecular alloys as phase
 145 change material. *Transfus Apher Sci* 2003;28:143–8. doi:10.1016/S1473-
 146 0502(03)00016-8.
- 147 17. Kalogirou S. The potential of solar industrial process heat applications. *Appl Energy*
 148 2003;76:337–61. doi:10.1016/S0306-2619(02)00176-9.
- 149 18. Schweiger H, Mendes JF, Benz N, Hennecke K, Prieto G, Cusi M, et al. The potential
 150 of solar heat in industrial processes. State of the art review for Spain and Portugal.
 151 ISES-Eur. Sol. Congr., Copenhagen, Denmark: 2000.
- 152 19. Pintaldi S, Perfumo C, Sethuvenkatraman S, White S, Rosengarten G. A review of
 153 thermal energy storage technologies and control approaches for solar cooling. *Renew*
 154 *Sustain Energy Rev* 2015;41:975–95. doi:10.1016/j.rser.2014.08.062.
- 155 20. Kenisarin M, Mahkamov K. Solar energy storage using phase change materials. *Renew*
 156 *Sustain Energy Rev* 2007;11:1913–65. doi:10.1016/j.rser.2006.05.005.
- 157 21. Medrano M, Gil A, Martorell I, Potau X, Cabeza LF. State of the art on high-
 158 temperature thermal energy storage for power generation. Part 2—Case studies. *Renew*
 159 *Sustain Energy Rev* 2010;14:56–72. doi:10.1016/j.rser.2009.07.036.
- 160 22. Pielichowska K, Pielichowski K. Phase change materials for thermal energy storage.
 161 *Prog Mater Sci* 2014;65:67–123. doi:10.1016/j.pmatsci.2014.03.005.
- 162 23. Gude VG. Energy storage for desalination processes powered by renewable energy and
 163 waste heat sources. *Appl Energy* 2015;137:877–98.
 164 doi:10.1016/j.apenergy.2014.06.061.
- 165 24. Gude VG, Nirmalakhandan N, Deng S. Renewable and sustainable approaches for
 166 desalination. *Renew Sustain Energy Rev* 2010;14:2641–54.
 167 doi:10.1016/j.rser.2010.06.008.
- 168 25. Nomura T, Okinaka N, Akiyama T. Technology of Latent Heat Storage for High
 169 Temperature Application: A Review. *ISIJ Int* 2010;50:1229–39.
 170 doi:10.2355/isijinternational.50.1229.

- 171 26. Brückner S, Liu S, Miró L, Radspieler M, Cabeza LF, Lävemann E. Industrial waste
172 heat recovery technologies: An economic analysis of heat transformation technologies.
173 *Appl Energy* 2015;151:157–67. doi:10.1016/j.apenergy.2015.01.147.
- 174 27. Zalba B, Marín JM, Cabeza LF, Mehling H. Review on thermal energy storage with
175 phase change: materials, heat transfer analysis and applications. *Appl Therm Eng*
176 2003;23:251–83. doi:10.1016/S1359-4311(02)00192-8.
- 177 28. Liu M, Saman W, Bruno F. Review on storage materials and thermal performance
178 enhancement techniques for high temperature phase change thermal storage systems.
179 *Renew Sustain Energy Rev* 2012;16:2118–32. doi:10.1016/j.rser.2012.01.020.
- 180 29. Cárdenas B, León N. Latent Heat Based High Temperature Solar Thermal Energy
181 Storage for Power Generation. *Energy Procedia* 2014;57:580–9.
182 doi:10.1016/j.egypro.2014.10.212.
- 183 30. Fernandes D, Pitié F, Cáceres G, Baeyens J. Thermal energy storage: “How previous
184 findings determine current research priorities.” *Energy* 2012;39:246–57.
185 doi:10.1016/j.energy.2012.01.024.
- 186 31. Abhat A. Low temperature latent heat thermal energy storage: Heat storage materials.
187 *Sol Energy* 1983;30:313–32. doi:10.1016/0038-092X(83)90186-X.
- 188 32. Dincer I, Rosen MA. *Thermal Energy Storage: Systems and Applications*. 2 edition.
189 Hoboken, N.J: Wiley; 2010.
- 190 33. Mehling H, Cabeza LF. *Heat and cold storage with PCM: An up to date introduction*
191 *into basics and applications*. Springer Science & Business Media; 2008.
- 192 34. Gasia J, Miró L, Cabeza LF. Materials and system requirements of high temperature
193 thermal energy storage systems: A review. Part 2: Thermal conductivity enhancement
194 techniques. *Renew Sustain Energy Rev* 2016;60:1584–601.
195 doi:10.1016/j.rser.2016.03.019.
- 196 35. Ferrer G, Solé A, Barreneche C, Martorell I, Cabeza LF. Corrosion of metal containers
197 for use in PCM energy storage. *Renew Energy* 2015;76:465–9.
198 doi:10.1016/j.renene.2014.11.036.
- 199 36. Solé A, Neumann H, Niedermaier S, Martorell I, Schossig P, Cabeza LF. Stability of
200 sugar alcohols as PCM for thermal energy storage. *Sol Energy Mater Sol Cells*
201 2014;126:125–34. doi:10.1016/j.solmat.2014.03.020.
- 202 37. John G, König-Haagen A, King’Ondu CK, Brüggemann D, Nkhonjera L. Galactitol as
203 phase change material for latent heat storage of solar cookers: Investigating thermal
204 behavior in bulk cycling. *Sol Energy* 2015;119:415–21.
205 doi:10.1016/j.solener.2015.07.003
- 206 38. Paul A, Shi L, Bielawski CW. A eutectic mixture of galactitol and mannitol as a phase
207 change material for latent heat storage. *Energy Convers Manag* 2015;103:139–46.
208 doi:10.1016/j.enconman.2015.06.013.
- 209 39. Sun JQ, Zhang RY, Liu ZP, Lu GH. Thermal reliability test of Al–34%Mg–6%Zn alloy
210 as latent heat storage material and corrosion of metal with respect to thermal cycling.
211 *Energy Convers Manag* 2007;48:619–24. doi:10.1016/j.enconman.2006.05.017.
- 212 40. Bauer T, Pflieger N, Breidenbach N, Eck M, Laing D, Kaesche S. Material aspects of
213 Solar Salt for sensible heat storage. *Appl Energy* 2013;111:1114–9.
214 doi:10.1016/j.apenergy.2013.04.072.
- 215 41. Guillot S, Faik A, Rakhmatullin A, Lambert J, Veron E, Echehut P, et al. Corrosion
216 effects between molten salts and thermal storage material for concentrated solar power
217 plants. *Appl Energy* 2012;94:174–81. doi:10.1016/j.apenergy.2011.12.057.
- 218 42. Fernández AG, Cortes M, Fuentealba E, Pérez FJ. Corrosion properties of a ternary
219 nitrate/nitrite molten salt in concentrated solar technology. *Renew Energy* 2015;80:177–
220 83. doi:10.1016/j.renene.2015.01.072.
- 221 43. Federsel K, Wortmann J, Ladenberger M. High-temperature and Corrosion Behavior of
222 Nitrate Nitrite Molten Salt Mixtures Regarding their Application in Concentrating Solar
223 Power Plants. *Energy Procedia* 2015;69:618–25. doi:10.1016/j.egypro.2015.03.071.
- 224 44. Fernández AG, Galleguillos H, Fuentealba E, Pérez FJ. Corrosion of stainless steels and
225 low-Cr steel in molten Ca(NO₃)₂–NaNO₃–KNO₃ eutectic salt for direct energy storage

- 226 in CSP plants. *Sol Energy Mater Sol Cells* 2015;141:7–13.
 227 doi:10.1016/j.solmat.2015.05.004.
- 228 45. Goods SH, Bradshaw RW. Corrosion of stainless steels and carbon steel by molten
 229 mixtures of commercial nitrate salts. *J Mater Eng Perform* 2004;13:78–87.
 230 doi:10.1361/10599490417542.
- 231 46. Slusser JW, Titcomb JB, Heffelfinger MT, Dunbobbin BR. Corrosion in Molten
 232 Nitrate-Nitrite Salts. *Jom* 1985;37:24–7. doi:10.1007/bf03259692
- 233 47. Fernández AG, Rey A, Lasanta I, Mato S, Brady MP, Pérez FJ. Corrosion of alumina-
 234 forming austenitic steel in molten nitrate salts by gravimetric analysis and impedance
 235 spectroscopy. *Mater Corros* 2014;65:267–75. doi:10.1002/maco.201307422.
- 236 48. Fernández AG, Galleguillos H, Pérez FJ. Thermal influence in corrosion properties of
 237 Chilean solar nitrates. *Sol Energy* 2014;109:125–34. doi:10.1016/j.solener.2014.07.027.
- 238 49. Fernández A, Grágeda M, Galleguillos H. Impurity Influence in Physico-chemical and
 239 Corrosion Properties of Chilean Solar Nitrates. *Energy Proced* 2014;49:607–16.
 240 doi:10.1016/j.egypro.2014.03.066.
- 241 50. Fernández AG, Lasanta MI, Pérez FJ. Molten Salt Corrosion of Stainless Steels and
 242 Low-Cr Steel in CSP Plants. *Oxid Met* 2012;78:329–48. doi:10.1007/s11085-012-9310-
 243 x.
- 244 51. Dorcheh AS, Durham RN, Galetz MC. Corrosion behavior of stainless and low-
 245 chromium steels and IN625 in molten nitrate salts at 600°C. *Sol Energy Mater Sol Cells*
 246 2016;144:109–16. doi:10.1016/j.solmat.2015.08.011.
- 247 52. Kruiženga A, Gill D. Corrosion of Iron Stainless Steels in Molten Nitrate Salt. *Energy*
 248 *Procedia* 2014;49:878–87. doi:10.1016/j.egypro.2014.03.095.
- 249 53. McConohy G, Kruiženga A. Molten nitrate salts at 600 and 680 °C: Thermophysical
 250 property changes and corrosion of high-temperature nickel alloys. *Sol Energy*
 251 2014;103:242–52. doi:10.1016/j.solener.2014.01.028.
- 252 54. Goods SH. Creep and the corrosion characteristics of Incoloy Alloy 800 in molten
 253 nitrate salts. *J Mater Energy Syst* 1981;3:43–50. doi:10.1007/BF02833528.
- 254 55. Cheng W-J, Chen D-J, Wang C-J. High-temperature corrosion of Cr–Mo steel in molten
 255 LiNO₃–NaNO₃–KNO₃ eutectic salt for thermal energy storage. *Sol Energy Mater Sol*
 256 *Cells* 2015;132:563–9. doi:10.1016/j.solmat.2014.10.007.
- 257 56. Sona CS, Gajbhiye BD, Hule PV, Patwardhan AW, Mathpati CS, Borgohain A, et al.
 258 High temperature corrosion studies in molten salt-FLiNaK. *Corros Eng Sci Technol*
 259 2013;49:287–95. doi:10.1179/1743278213Y.0000000135.
- 260 57. Li Y, Spiegel M, Shimada S. Corrosion behaviour of various model alloys with NaCl–
 261 KCl coating. *Mater Chem Phys* 2005;93:217–23.
 262 doi:10.1016/j.matchemphys.2005.03.015.
- 263 58. Abramov AV, Polovov IB, Volkovich VA, Rebrin OI, Griffiths TR, May I, et al.
 264 Spectroelectrochemical Study of Stainless Steel Corrosion in NaCl-KCl Melt. *ECS*
 265 *Trans* 2010;33:277-85. doi:10.1149/1.3484785.
- 266 59. Vignarooban K, Xu X, Wang K, Molina E, Li P, Gervasio D, et al. Vapor pressure and
 267 corrosivity of ternary metal-chloride molten-salt based heat transfer fluids for use in
 268 concentrating solar power systems. *Appl Energ* 2015;159:206–13.
 269 doi:10.1016/j.apenergy.2015.08.131.
- 270 60. Miró L, Barreneche C, Ferrer G, Solé A, Martorell I, Cabeza LF. Health hazard, cycling
 271 and thermal stability as key parameters when selecting a suitable phase change material
 272 (PCM). *Thermochim Acta* 2016;627-629:39–47. doi:10.1016/j.tca.2016.01.014.
- 273 61. Gallegos MA, Yu W. Thermal performance and flammability of phase change material
 274 for medium and elevated temperatures for textile application. *J Therm Anal Calorim*
 275 2014;117:9–17. doi:10.1007/s10973-013-3411-x.
- 276 62. Zhao W. Characterization of Encapsulated Phase Change Materials for Thermal Energy
 277 Storage. Lehigh University, 2013.
- 278 63. Nath R. Encapsulation of High Temperature Phase Change Materials for Thermal
 279 Energy Storage. Grad Theses Diss 2012.

- 280 64. Pitié F, Zhao CY, Cáceres G. Thermo-mechanical analysis of ceramic encapsulated
281 phase-change-material (PCM) particles. *Energy Environ Sci* 2011;4:2117–24.
282 doi:10.1039/C0EE00672F.
- 283 65. Fukahori R, Nomura T, Zhu C, Sheng N, Okinaka N, Akiyama T. Macro-encapsulation
284 of metallic phase change material using cylindrical-type ceramic containers for high-
285 temperature thermal energy storage. *Appl Energy* 2016;170:324–8.
286 doi:10.1016/j.apenergy.2016.02.106.
- 287 66. Jacob R, Bruno F. Review on shell materials used in the encapsulation of phase change
288 materials for high temperature thermal energy storage. *Renew Sust Energ Rev*
289 2015;48:79–87. doi:10.1016/j.rser.2015.03.038
- 290 67. Legay M, Gondrexon N, Le Person S, Boldo P, Bontemps A. Enhancement of Heat
291 Transfer by Ultrasound: Review and Recent Advances. *Int J Chem Eng*
292 2011;2011:e670108. doi:10.1155/2011/670108.
- 293 68. Sarı A, Biçer A, Lafçı Ö, Ceylan M. Galactitol hexa stearate and galactitol hexa
294 palmitate as novel solid–liquid phase change materials for thermal energy storage. *Sol*
295 *Energy* 2011;85:2061–71. doi:10.1016/j.solener.2011.05.014.
- 296 69. Rathgeber C, Miró L, Cabeza LF, Hiebler S. Measurement of enthalpy curves of phase
297 change materials via DSC and T-History: When are both methods needed to estimate
298 the behaviour of the bulk material in applications? *Thermochim Acta* 2014;596:79–88.
299 doi:10.1016/j.tca.2014.09.022.
- 300 70. Gil A, Oró E, Peiró G, Álvarez S, Cabeza LF. Material selection and testing for thermal
301 energy storage in solar cooling. *Renew Energy* 2013;57:366–71.
302 doi:10.1016/j.renene.2013.02.008.
- 303 71. Rathgeber C, Schmit H, Miró L, Cabeza LF, Gutierrez A, Ushak S. Analysis of
304 subcooling of phase change materials with increased sample size - Comparison of
305 measurements via DSC, T-History and at pilot plant scale. 13h Int. Conf. Therm.
306 Energy Storage, Beijing, China: 2015.
- 307 72. Archibold AR, Gonzalez-Aguilar J, Rahman MM, Yogi Goswami D, Romero M,
308 Stefanakos EK. The melting process of storage materials with relatively high phase
309 change temperatures in partially filled spherical shells. *Appl Energy* 2014;116:243–52.
310 doi:10.1016/j.apenergy.2013.11.048.
- 311 73. Solomon L, Elmozughi, Oztekin A. Effect of Internal Void Placement on Heat Transfer
312 Performance – Encapsulated Phase Change material for Energy Storage. *Renew Energy*
313 2015;78:438–47. doi:10.1016/j.renene.2015.01.035.
- 314 74. Hennemann P, Hiebler S, Hauer A. Physical limitations to the usage of PCM - A
315 theoretical approach. 13h Int. Conf. Therm. Energy Storage, Beijing, Xina: 2015.
- 316 75. Andreu-Cabedo P, Mondragon R, Hernandez L, Martinez-Cuenca R, Cabedo L, Julia
317 JE. Increment of specific heat capacity of solar salt with SiO₂ nanoparticles. *Nanoscale*
318 *Res Lett* 2014;9:582. doi:10.1186/1556-276X-9-582.
- 319 76. Shin D, Banerjee D. Enhancement of specific heat capacity of high-temperature silica-
320 nanofluids synthesized in alkali chloride salt eutectics for solar thermal-energy storage
321 applications. *Int J Heat Mass Transf* 2011;54:1064–70.
322 doi:10.1016/j.ijheatmasstransfer.2010.11.017.
- 323 77. Ho MX, Pan C. Optimal concentration of alumina nanoparticles in molten Hitec salt to
324 maximize its specific heat capacity. *Int J Heat Mass Transf* 2014;70:174–84.
325 doi:10.1016/j.ijheatmasstransfer.2013.10.078.
- 326 78. Shahrul IM, Mahbulul IM, Khaleduzzaman SS, Saidur R, Sabri MFM. A comparative
327 review on the specific heat of nanofluids for energy perspective. *Renew Sustain Energy*
328 *Rev* 2014;38:88–98. doi:10.1016/j.rser.2014.05.081.
- 329 79. Shin D, Banerjee D. Enhancement of Heat Capacity of Molten Salt Eutectics using
330 Inorganic Nanoparticles for Solar Thermal Energy Applications. In: Kriven WM,
331 Gyekenyesi AL, Wang J, Widjaja S, Singh D, editors. *Dev. Strateg. Mater. Comput.*
332 *Des. II*, John Wiley & Sons, Inc.; 2011, p. 119–26.

- 333 80. Lazaro A, Peñalosa C, Solé A, Diarce G, Haussmann T, Fois M, et al. Intercomparative
334 tests on phase change materials characterisation with differential scanning calorimeter.
335 *Appl Energy* 2013;109:415–20. doi:10.1016/j.apenergy.2012.11.045.
- 336 81. Jung S, Banerjee D. Enhancement of Heat Capacity of Nitrate Salts using Mica
337 Nanoparticles. In: Kriven WM, Gyekenyesi AL, Wang J, Widjaja S, Singh D, editors.
338 *Dev. Strateg. Mater. Comput. Des. II*, John Wiley & Sons, Inc.; 2011, p. 127–37.
- 339 82. Chieruzzi M, Cerritelli GF, Miliozzi A, Kenny JM. Effect of nanoparticles on heat
340 capacity of nanofluids based on molten salts as PCM for thermal energy storage.
341 *Nanoscale Res Lett* 2013;8:448. doi:10.1186/1556-276X-8-448.
- 342 83. Dudda B, Shin D. Effect of nanoparticle dispersion on specific heat capacity of a binary
343 nitrate salt eutectic for concentrated solar power applications. *Int J Therm Sci*
344 2013;69:37–42. doi:10.1016/j.ijthermalsci.2013.02.003.
- 345 84. Lu M-C, Huang C-H. Specific heat capacity of molten salt-based alumina nanofluid.
346 *Nanoscale Res Lett* 2013;8:292. doi:10.1186/1556-276X-8-292.
- 347 85. Schuller M, Shao Q, Lalk T. Experimental investigation of the specific heat of a nitrate–
348 alumina nanofluid for solar thermal energy storage systems. *Int J Therm Sci*
349 2015;91:142–5. doi:10.1016/j.ijthermalsci.2015.01.012.
- 350 86. Chieruzzi M, Miliozzi A, Crescenzi T, Torre L, Kenny JM. A New Phase Change
351 Material Based on Potassium Nitrate with Silica and Alumina Nanoparticles for
352 Thermal Energy Storage. *Nanoscale Res Lett* 2015;10.
353 doi:10.1186/s11671-015-0984-2.
- 354 87. Tao YB, Lin CH, He YL. Preparation and thermal properties characterization of
355 carbonate salt/carbon nanomaterial composite phase change material. *Energy Convers*
356 *Manag* 2015;97:103–10. doi:10.1016/j.enconman.2015.03.051.
- 357 88. Seo J, Shin D. Size effect of nanoparticle on specific heat in a ternary nitrate (LiNO₃–
358 NaNO₃–KNO₃) salt eutectic for thermal energy storage. *Applied Thermal Engineering*
359 2016;102:144–8. doi:10.1016/j.applthermaleng.2016.03.134.
- 360 89. Lai C-C, Chang W-C, Hu W-L, Wang ZM, Lu M-C, Chueh Y-L. A solar-thermal
361 energy harvesting scheme: enhanced heat capacity of molten HITEC salt mixed with
362 Sn/SiO_x core-shell nanoparticles. *Nanoscale* 2014;6:4555–9.
363 doi:10.1039/C3NR06810B.
- 364 90. Bridges NJ, Visser AE, Fox EB. Potential of nanoparticle enhanced ionic liquids
365 (NEILs) as advanced heat-transfer fluids. *Energy Fuels* 2011;25:4862–4.
- 366 91. Shin D, Banerjee D. Experimental Investigation of Molten Salt Nanofluid for Solar
367 Thermal Energy Application 2011:T30024–T30024. doi:10.1115/AJTEC2011-44375.
- 368 92. Shin D, Banerjee D. Enhanced Specific Heat Capacity of Nanomaterials Synthesized by
369 Dispersing Silica Nanoparticles in Eutectic Mixtures. *J Heat Transf* 2013;135:032801–
370 032801. doi:10.1115/1.4005163.
- 371 93. Tiznobaik H, Shin D. Enhanced specific heat capacity of high-temperature molten salt-
372 based nanofluids. *Int J Heat Mass Transf* 2013;57:542–8.
373 doi:10.1016/j.ijheatmasstransfer.2012.10.062.
- 374 94. Seo J, Shin D. Enhancement of specific heat of ternary nitrate (LiNO₃-NaNO₃-KNO₃)
375 salt by doping with SiO₂ nanoparticles for solar thermal energy storage. *IET Micro*
376 *Nano Lett* 2014;9:817–20. doi:10.1049/mnl.2014.0407.
- 377 95. Shin D, Banerjee D. Specific heat of nanofluids synthesized by dispersing alumina
378 nanoparticles in alkali salt eutectic. *Int J Heat Mass Transf* 2014;74:210–4.
379 doi:10.1016/j.ijheatmasstransfer.2014.02.066.
- 380 96. Jo B, Banerjee D. Effect of Dispersion Homogeneity on Specific Heat Capacity
381 Enhancement of Molten Salt Nanomaterials Using Carbon Nanotubes. *J Sol Energy*
382 *Eng* 2014;137:011011–011011. doi:10.1115/1.4028144.
- 383 97. Shin D, Banerjee D. Enhanced thermal properties of SiO₂ nanocomposite for solar
384 thermal energy storage applications. *Int J Heat Mass Transf* 2015;84:898–902.
385 doi:10.1016/j.ijheatmasstransfer.2015.01.100.

- 386 98. Devaradjane R, Shin D. Nanoparticle Dispersions on Ternary Nitrate Salts for Heat
387 Transfer Fluid Applications in Solar Thermal Power. *J Heat Transfer Journal Of Heat*
388 *Transfer* 2016;138:051901. doi:10.1115/1.4030903
- 389 99. Vignarooban K, Xu X, Arvay A, Hsu K, Kannan AM. Heat transfer fluids for
390 concentrating solar power systems – A review. *Appl Energy* 2015;146:383–96.
391 doi:10.1016/j.apenergy.2015.01.125.
- 392 100. Liu M, Belusko M, Steven Tay NH, Bruno F. Impact of the heat transfer fluid in
393 a flat plate phase change thermal storage unit for concentrated solar tower plants. *Sol*
394 *Energy* 2014;101:220–31. doi:10.1016/j.solener.2013.12.030.
- 395 101. Heller L. Literature Review on Heat Transfer Fluids and Thermal Energy
396 Storage Systems in CSP Plants. STERG Report 2013.
- 397 102. Pacio J, Wetzel T. Assessment of liquid metal technology status and research
398 paths for their use as efficient heat transfer fluids in solar central receiver systems. *Sol*
399 *Energy* 2013;93:11–22. doi:10.1016/j.solener.2013.03.025.
- 400 103. Cingarapu S, Singh D, Timofeeva EV, Moravek MR. Nanofluids with
401 encapsulated tin nanoparticles for advanced heat transfer and thermal energy storage.
402 *Int J Energy Res* 2014;38:51–9. doi:10.1002/er.3041.
- 403 104. Torres-Mendieta R, Mondragón R, Juliá E, Mendoza-Yero O, Cordoncillo E,
404 Lancis J, et al. Fabrication of gold nanoparticles in Therminol VP-1 by laser ablation
405 and fragmentation with fs pulses. *Laser Phys Lett Laser Physics Letters*
406 2014;11:126001. doi:10.1088/1612-2011/11/12/126001
- 407 105. Boissiere B, Ansart R, Gauthier D, Flamant G, Hemati M. Experimental
408 hydrodynamic study of gas-particle dense suspension upward flow for application as
409 new heat transfer and storage fluid. *Can J Chem Eng* 2015;93:317–30.
410 doi:10.1002/cjce.22087
- 411 106. International Renewable Energy Agency. Renewable energy technologies: Cost
412 analysis series. Volume 1: Power Sector. Issue 2/5 Concentrating solar power 2012.
- 413 107. International Energy Agency. Technology Roadmap: Concentrating solar power
414 2010.
- 415 108. Fichtner GmbH & Co. Technology Assessment of CSP Technologies for a Site
416 Specific Project in South Africa Final Report, The World Bank and ESMAP,
417 Washington D.C. 2010.
- 418 109. Wagner SJ, Rubin ES. Economic implications of thermal energy storage for
419 concentrated solar thermal power. *Renew Energy* 2014;61:81–95.
420 doi:10.1016/j.renene.2012.08.013.
- 421 110. Nithyanandam K, Pitchumani R. Cost and performance analysis of
422 concentrating solar power systems with integrated latent thermal energy storage. *Energy*
423 2014;64:793–810. doi:10.1016/j.energy.2013.10.095.
- 424 111. Rathgeber C, Hiebler S, Lävemann E, Hauer A. Economic Evaluation of
425 Thermal Energy Storages via Top-down and Bottom-up Approach. 13h Int. Conf.
426 Therm. Energy Storage, Beijing, China: 2015.
- 427 112. Carbon Trust. Carbon footprinting guide 2015.
428 [http://www.carbontrust.com/resources/guides/carbon-footprinting-and-](http://www.carbontrust.com/resources/guides/carbon-footprinting-and-reporting/carbon-footprinting)
429 [reporting/carbon-footprinting.](http://www.carbontrust.com/resources/guides/carbon-footprinting-and-reporting/carbon-footprinting)
- 430 113. Hirschier R, Weidema B. Implementation of Life Cycle Impact Assessment
431 Methods. ecoinvent report No. 3, v2.2 2010.
- 432 114. IHOBE, Sociedad Pública de Gestión Ambiental. Análisis de ciclo de vida y
433 huella de carbono. Dos maneras de medir el impacto ambiental de un producto. 2009.
- 434 115. Khare S, Dell’Amico M, Knight C, McGarry S. Selection of materials for high
435 temperature sensible energy storage. *Sol Energy Mater Sol Cells* 2013;115:114–22.
436 doi:10.1016/j.solmat.2013.03.009.
- 437 116. López-Sabirón AM, Royo P, Ferreira VJ, Aranda-Usón A, Ferreira G. Carbon
438 footprint of a thermal energy storage system using phase change materials for industrial
439 energy recovery to reduce the fossil fuel consumption. *Appl Energy* 2014;135:616–24.
440 doi:10.1016/j.apenergy.2014.08.038.

- 441 117. López-Sabirón AM, Aranda-Usón A, Mainar-Toledo MD, Ferreira VJ, Ferreira
442 G. Environmental profile of latent energy storage materials applied to industrial
443 systems. *Sci Total Environ* 2014;473–474:565–75. doi:10.1016/j.scitotenv.2013.12.013.
- 444 118. Oró E, Gil A, de Gracia A, Boer D, Cabeza LF. Comparative life cycle
445 assessment of thermal energy storage systems for solar power plants. *Renew Energy*
446 2012;44:166–73. doi:10.1016/j.renene.2012.01.008.
- 447 119. Miró L, Oró E, Boer D, Cabeza LF. Embodied energy in thermal energy storage
448 (TES) systems for high temperature applications. *Appl Energy* 2015;137:793–9.
449 doi:10.1016/j.apenergy.2014.06.062.
- 450 120. Lalau Y, Py X, Meffre A, Olives R. Comparative LCA Between Current and
451 Alternative Waste-Based TES for CSP. *Waste Biomass Valor Waste And Biomass*
452 *Valorization* 2016. doi:10.1007/s12649-016-9549-6.
- 453 121. Klein SJW. Multi-Criteria Decision Analysis of Concentrated Solar Power with
454 Thermal Energy Storage and Dry Cooling. *Environ Sci Technol* 2013;47:13925–33.
455 doi:10.1021/es403553u.
- 456 122. Klein SJW, Rubin ES. Life cycle assessment of greenhouse gas emissions,
457 water and land use for concentrated solar power plants with different energy backup
458 systems. *Energy Policy* 2013;63:935–50. doi:10.1016/j.enpol.2013.08.057.
- 459 123. Lechón Y, de la Rúa C, Sáez R. Life Cycle Environmental Impacts of
460 Electricity Production by Solarthermal Power Plants in Spain. *J Sol Energy Eng*
461 2008;130:021012–021012. doi:10.1115/1.2888754.
- 462 124. Giuliano S, Buck R, Eguiguren S. Analysis of Solar-Thermal Power Plants
463 With Thermal Energy Storage and Solar-Hybrid Operation Strategy. *J Sol Energy Eng*
464 2011;133:031007–031007. doi:10.1115/1.4004246.
- 465 125. Whitaker MB, Heath GA, Burkhardt JJ, Turchi CS. Life Cycle Assessment of a
466 Power Tower Concentrating Solar Plant and the Impacts of Key Design Alternatives.
467 *Environ Sci Technol* 2013;47:5896–903. doi:10.1021/es400821x.
- 468 126. Burkhardt JJ, Heath GA, Turchi CS. Life Cycle Assessment of a Parabolic
469 Trough Concentrating Solar Power Plant and the Impacts of Key Design Alternatives.
470 *Environ Sci Technol* 2011;45:2457–64. doi:10.1021/es1033266.
- 471 127. Gutierrez A, Miró L, Gil A, Rodríguez-Aseguinolaza J, Barreneche C, Calvet
472 N, et al. Advances in the valorization of waste and by-product materials as thermal
473 energy storage (TES) materials. *Renew Sustain Energy Rev* 2016;59:763–83.
474 doi:10.1016/j.rser.2015.12.071.
- 475 128. Py X, Calvet N, Olives R, Meffre A, Echegut P, Bessada C, et al. Recycled
476 Material for Sensible Heat Based Thermal Energy Storage to be Used in Concentrated
477 Solar Thermal Power Plants. *J Sol Energy Eng* 2011;133:031008–031008.
478 doi:10.1115/1.4004267.
- 479 129. Kere A, Sadiki N, Py X, Goetz V. Applicability of thermal energy storage
480 recycled ceramics to high temperature and compressed air operating conditions. *Energy*
481 *Convers Manag* 2014;88:113–9. doi:10.1016/j.enconman.2014.08.008.
- 482 130. Gualtieri AF, Tartaglia A. Thermal decomposition of asbestos and recycling in
483 traditional ceramics. *J Eur Ceram Soc* 2000;20:1409–18. doi:10.1016/S0955-
484 2219(99)00290-3.
- 485 131. Calvet N, Gomez JC, Faik A, Roddatis VV, Meffre A, Glatzmaier GC, et al.
486 Compatibility of a post-industrial ceramic with nitrate molten salts for use as filler
487 material in a thermocline storage system. *Appl Energy* 2013;109:387–93.
488 doi:10.1016/j.apenergy.2012.12.078.
- 489 132. Meffre A, Py X, Olives R, Bessada C, Veron E, Echegut P. High-Temperature
490 Sensible Heat-Based Thermal Energy Storage Materials Made of Vitrified MSWI Fly
491 Ashes. *Waste Biomass Valor Waste And Biomass Valorization* 2015;6:1003–14.
492 doi:10.1007/s12649-015-9409-9.
- 493 133. Faik A, Guillot S, Lambert J, Véron E, Ory S, Bessada C, et al. Thermal storage
494 material from inertized wastes: Evolution of structural and radiative properties with
495 temperature. *Sol Energy* 2012;86:139–46. doi:10.1016/j.solener.2011.09.014.

- 496 134. Miró L, Navarro ME, Suresh P, Gil A, Fernández AI, Cabeza LF. Experimental
497 characterization of a solid industrial by-product as material for high temperature
498 sensible thermal energy storage (TES). *Appl Energy* 2014;113:1261–8.
499 doi:10.1016/j.apenergy.2013.08.082.
- 500 135. Ushak S, Gutierrez A, Flores E, Galleguillos H, Grageda M. Development of
501 Thermal Energy Storage Materials from Waste-process Salts. *Energy Procedia*
502 2014;57:627–32. doi:10.1016/j.egypro.2014.10.217.
- 503 136. Calvet N, Dejean G, Unamunzaga L, Py X. Waste From Metallurgic Industry: A
504 Sustainable High-Temperature Thermal Energy Storage Material for Concentrated Solar
505 Power 2013;V001T03A012. doi:10.1115/ES2013-18333.
- 506 137. Ozger OB, Girardi F, Giannuzzi GM, Salomoni VA, Majorana CE, Fambri L, et
507 al. Effect of nylon fibres on mechanical and thermal properties of hardened concrete for
508 energy storage systems. *Mater Des* 2013;51:989–97. doi:10.1016/j.matdes.2013.04.085.
- 509 138. Navarro ME, Martínez M, Gil A, Fernández AI, Cabeza LF, Olives R, et al.
510 Selection and characterization of recycled materials for sensible thermal energy storage.
511 *Sol Energy Mater Sol Cells* 2012;107:131–5. doi:10.1016/j.solmat.2012.07.032.
- 512 139. Gil A, Olives R, Faure R, Tessier-Doyen, Huger M. Thermomechanical
513 characterization of recycled high temperature thermal energy storage material. *Adv.*
514 *Therm. Energy Storage Technol.*, Lleida, Spain: 2014.
- 515 140. Ortega I, Faik A, Gil A, Rodriguez-Aseguinolaza J, D’Aguanno B. Thermo-
516 physical properties of a Steel-making by-product to be used as thermal energy storage
517 material in a packed-bed system. *Conc. Sol. Power Chem. Energy Syst.*, Beijing, China:
518 2014.
- 519 141. Ortega I, Rodriguez-Aseguinolaza J, Gil A, Faik A, D’Aguanno B. New thermal
520 energy storage materials from industrial wastes: compatibility of Steel slags with the
521 most common heat transfer fluids. *Int. Conf. Energy Sustain.*, Boston, USA: 2012.
- 522 142. Mills K. The estimation of slag properties, *Cradle of Humankind*, South Africa:
523 2011.
- 524 143. Peiró G, Gasia J, Miró L, Cabeza LF. Experimental evaluation at pilot plant
525 scale of multiple PCMs (cascaded) vs. single PCM configuration for thermal energy
526 storage. *Renew Energy* 2015;83:729–36. doi:10.1016/j.renene.2015.05.029.
- 527 144. Tao YB, He YL, Liu YK, Tao WQ. Performance optimization of two-stage
528 latent heat storage unit based on entransy theory. *Int J Heat Mass Transf* 2014;77:695–
529 703. doi:10.1016/j.ijheatmasstransfer.2014.05.049.
- 530 145. Li YQ, He YL, Song HJ, Xu C, Wang WW. Numerical analysis and parameters
531 optimization of shell-and-tube heat storage unit using three phase change materials.
532 *Renew Energy* 2013;59:92–9. doi:10.1016/j.renene.2013.03.022.
- 533 146. Gong Z-X, Mujumdar AS. A New Solar Receiver Thermal Store for Space-
534 Based Activities Using Multiple Composite Phase-Change Materials. *J Sol Energy Eng*
535 1995;117:215–20. doi:10.1115/1.2847798.
- 536 147. Cui H, Yuan X, Hou X. Thermal performance analysis for a heat receiver using
537 multiple phase change materials. *Appl Therm Eng* 2003;23:2353–61.
538 doi:10.1016/S1359-4311(03)00210-2.
- 539 148. Michels H, Pitz-Paal R. Cascaded latent heat storage for parabolic trough solar
540 power plants. *Sol Energy* 2007;81:829–37. doi:10.1016/j.solener.2006.09.008.
- 541 149. Seeniraj RV, Lakshmi Narasimhan N. Performance enhancement of a solar
542 dynamic LHTS module having both fins and multiple PCMs. *Sol Energy* 2008;82:535–
543 42. doi:10.1016/j.solener.2007.11.001.
- 544 150. Shabgard H, Robak CW, Bergman TL, Faghri A. Heat transfer and exergy
545 analysis of cascaded latent heat storage with gravity-assisted heat pipes for
546 concentrating solar power applications. *Sol Energy* 2012;86:816–30.
547 doi:10.1016/j.solener.2011.12.008.
- 548 151. Wang P, Wang X, Huang Y, Li C, Peng Z, Ding Y. Thermal energy charging
549 behaviour of a heat exchange device with a zigzag plate configuration containing multi-

- 550 phase-change-materials (m-PCMs). Appl Energy 2015;142:328–36.
551 doi:10.1016/j.apenergy.2014.12.050.
- 552 152. Gasia J, Tay NHS, Bruno F, Cabeza LF, Belusko M. Experimental investigation
553 of the effect of dynamic melting in a cylindrical shell-and-tube heat exchanger using
554 water as PCM. Applied Energy. Submitt to Appl Energ n.d.
- 555 153. Tay NHS, Bruno F, Belusko M. Experimental investigation of dynamic melting
556 in a tube-in-tank PCM system. Appl Energy 2013;104:137–48.
557 doi:10.1016/j.apenergy.2012.11.035.
- 558 154. Zipf V, Neuhäuser A, Willert D, Nitz P, Gschwander S, Platzer W. High
559 temperature latent heat storage with a screw heat exchanger: Design of prototype. Appl
560 Energ 2013;109:462–9. doi:10.1016/j.apenergy.2012.11.044
- 561 155. Pointner H, Steinmann W-D. Experimental demonstration of an active latent
562 heat storage concept. Applied Energy 2016;168:661–71.
563 doi:10.1016/j.apenergy.2016.01.113